Electronic Supplementary Material (ESI) for Materials Chemistry Frontiers.

Supporting Information

Acetylene bridged alkoxyphenanthrene and triarylamine-based triads for low threshold voltage with high mobility OFETs

Balu Balambiga, [a] Paneerselvam Devibala, [a] Deivendran Harshini, [a] Predhanekar Mohamed Imran, [b] and Samuthira Nagarajan*[a]

[a] Organic Electronics Division, Department of Chemistry, Central University of Tamil Nadu, Thiruvarur 610 005, India.

[b] Department of Chemistry, Islamiah College, Vaniyambadi 635 752, India.

General information

Materials and Methods

9,10-Phenanthroquinone, N-iodoscuccinimide (NIS), trifluoromethane sulfonic acid, hexyl bromide, $Na_2S_2O_4$, triphenylamine, N-bromosuccinamide (NBS), $POCl_3$, 4-tert-butylphenylboronic acid, potassium iodide, potassium iodate, $Pd(PPh_3)_2Cl_2$, copper iodide, $Pd(PPh_3)_4$ were purchased from the commercial sources. Anhydrous tetrahydrofuran (THF), N, N- dimethylformamide (DMF), trimethylamine (TEA), acetic acid, and carbon tetrachloride (CCl_4) were obtained from the Merck and used without any further purification. For spectrochemical analysis, ACS-grade solvents were used as received. Progress of the reaction was monitored by thin-layer chromatography (TLC) using standard TLC silica gel plates and examined with UV light. The compounds were purified with column chromatography using 100−200 mesh silica gel. ^1H and ^{13}C NMR spectra were recorded in Bruker 400 MHz spectrometer using tetramethylsilane (TMS) as internal standard and $CDCl_3$ as solvent. High-resolution mass spectra were obtained from Thermo Exactive Plus UHPLC-MS. Absorption and emission spectra were recorded using the JASCO UV-NIR spectrophotometer and Perkin-Elmer LS 55 spectrophotometer, respectively. Electrochemical studies were performed with CH Instruments (CHI 6035D). A conventional cell setup containing three electrodes was used with glassy carbon (working electrode), a standard calomel electrode (reference), and a platinum wire as the counter electrode was used in an anhydrous dichloromethane solvent with tetrabutylammonium hexafluorophosphate (TBAPF6) as a supporting electrolyte. The system was standardized externally using Fc/Fc^+. Thermal analyses were carried out in TA thermal analyzer under nitrogen gas flow with a scan rate of 10˚C per minute. SEM measurements were performed with a VEGA 3 TESCAN microscopy. Grazing incidence X-ray diffraction was performed in the reflection mode (CuK_α radiation) by an XPERT-PRO X-Ray diffractometer. DFT studies were employed to analyze the geometry and energy levels of the molecules. OFET characterizations were carried out using Keithley 4200-A semiconductor parameter analyzer at ambient conditions.

SYNTHESIS OF COMPOUNDS

Compound 1a: Phenanthrene-9,10-dione (6.0 g, 28.8 mmol, 1.0 eq.) in trifluoromethanesulfonic acid (30 mL) was cooled to 0 °C. N-Iodosuccinimide (19.5 g, 86.4 mmol, 3.0 eq.) was added slowly to the reaction mixture for 30 minutes. Then it was allowed to settle down to room temperature, and the content was added over H_2O/ice to induce the precipitation. The orange solid was recrystallized from $CHCl_3$.[1] The mixture of diiodophenanthrene-9,10 dione (5 g, 24.0 mmol), $Na_2S_2O_4$ (22.78 g, 144 mmol), and Bu_4NBr (4.64 g, 14.4 mmol) in 200 mL THF: H_2O (1:1, v/v) was stirred for 15 mins at room temperature. To this mixture, hexyl bromide (17.95 g, 72 mmol) followed by aqueous KOH (20 g, 360 mmol, in 100 mL of H_2O) was added slowly, and it was allowed to stir for a further 48 hours. The reaction mixture was diluted with 150 mL of water and then extracted with ethyl acetate (200 mL × 2). The combined organic layer was washed with water and brine then the solvent was removed under low pressure. The crude was recrystallized from methanol to yield compound **1a** as a white solid (yield 75 %). ^1H NMR (400 MHz, $CDCl_3$) δ (ppm) 8.58 (d, *J* = 1.6 Hz, 2H), 8.26 (S, 2H), 7.86 (d, *J* = 8.8 Hz, 2H), 4.19-4.16 (t, *J* = 6.8 Hz, 4H), 1.92 – 1.85 (m, 4H), 1.42-1.37 (m, 8H), 1.30-1.24 (m, 4H), 0.96 – 0.92 (m, 6H). ^{13}C NMR (100 MHz, $CDCl_3$) δ(ppm) 142.51, 134.54, 131.39, 127.16, 123.96, 93.28, 73.61, 31.60, 30.33, 29.68, 25.85, 22.72, 14.10

Compound 1b: Phenanthrene-9,10-dione (6.0 g, 28.8 mmol, 1.0 eq.) in trifluoromethanesulfonic acid (30 mL) was cooled to 0 °C. N-Iodosuccinimide (9.75 g, 43.2 mmol, 1.5 eq.) was added slowly to the reaction mixture for 30 minutes. Then it was allowed to settle down to room temperature and the content was added over H_2O to induce the precipitation. 2-Diiodophenanthrene-9,10-dione was recrystallized from $CHCl_3$. A mixture of 2-monoiodophenanthrene-9,10-dione (5 g, 24.0 mmol), $Na_2S_2O_4$ (22.78 g, 144 mmol), and Bu_4NBr (4.64 g, 14.4 mmol) in 200 mL THF: H_2O (1:1, v/v) was stirred for 15 mins at room temperature. To this mixture, n-hexyl bromide (8.98 g, 36 mmol) followed by aqueous KOH (20 g, 360 mmol, in 100 mL of H_2O) was added slowly and allowed to stir for another 48 hours. The reaction mixture was diluted with 150 mL of water and then extracted with ethyl acetate (200 mL × 2). The combined organic layer was washed with water, and brine then the solvent was removed under a vacuum. The crude recrystallized from methanol to yield compound **1b.** White solid (yield, 65 %). ^{1}H NMR (400 MHz, $CDCl_3$) δ(ppm) 8.55 – 8.40 (m, 2H), 8.18 (d, 8.0 Hz, 2H), 7.75 (d, *J* = 8.0 Hz, 2H), 7.52 (s, 1H), 4.72 – 4.07 (m, 4H), 1.86 – 1.77 (m, 4H), 1.51 – 1.45 (m, 4H), 1.34 – 1.26 (m, 8H), 0.86 (dd, *J* = 7.5, 6.5 Hz, 6H). ^{13}C NMR (100 MHz, $CDCl_3$) δ (ppm) 143.47, 142.53, 141.57, 134.79, 133.82, 131.45, 129.61, 128.17, 127.68, 127.26, 126.00, 124.43, 123.97, 122.28, 92.91, 92.64, 73.37, 31.22, 30.06, 25.86, 22.74, 14.32.

General procedure for Sonogashira coupling: In a two-necked round-bottomed flask, aryl iodide in dry THF (10 mL) and Et_3N (20 mL), followed by $PdCl_2(PPh_3)_2$ (0.05 mol %), CuI (0.05 mol %) were taken under nitrogen. Corresponding acetylene was introduced after 10 minutes. After the completion of the reaction, the organic phase was separated using dichloromethane, and the solvent was removed under reduced pressure.[2][3] The crude was purified by column chromatography on silica gel.

General procedure for trimethylsilyl deprotection: The resultant product from the Sonogashira reaction was dissolved in THF: methanol and allowed to react with K_2CO_3 under room temperature for 2-4 hours. The reaction mixture was poured over water and extracted with dichloromethane. The combined organic phase was dried over anhydrous Na_2SO_4, and the solvent was removed under a vacuum. The residue was purified by column chromatography on silica gel to afford the pure product.

Compound 2: Compound **1b** (1 g, 3.09 mmol) was allowed to react with trimethylsilylacetylene (1.32 ml, 9.28 mmol) at room temperature for 5 hours, and the resultant product (0.65 g, 1.92 mmol) was stirred with K_2CO_3 (0.8 g, 5.8 mmol) for 2 hours as per the general procedure for trimethylsilyl deprotection to give compound **2.** Colorless semisolid (yield 62 %). ^{1}H NMR (400 MHz, $CDCl_3$) δ (ppm) 8.57 (t, *J* = 8.9 Hz, 2H), 8.39 (d, *J* = 1.5 Hz, 1H), 8.24 (dd, *J* = 7.1, 2.3 Hz, 1H), 7.68 – 7.58 (m, 3H), 4.20 (t, *J* = 6.7 Hz, 4H), 3.18 (s, 1H), 1.95 – 1.85 (m, 4H), 1.56 (s, 4H), 1.39 (m, 8H), 0.93 (m, 6H). ^{13}C NMR (100 MHz, $CDCl_3$) δ (ppm) 143.73, 142.53, 130.04, 129.40, 128.57, 127.19, 126.53, 125.93, 122.83, 122.74, 122.37, 120.14, 84.19, 77.47, 73.72, 31.73, 30.45, 25.88, 22.65, 14.04.

Compound 3: To a solution of triphenylamine (1.5 g, 6 mmol) in CCl_4 (35 mL), N-bromosuccinimide (1.07 g, 6 mmol) was added and refluxed at 70°C for 4 hours. The crude mixture was cooled to ambient temperature and filtered. The residue was recrystallized from ethanol to afford the pure product. Colorless solid (yield, 90 %). ^{1}H NMR (400 MHz, $CDCl_3$) δ (ppm) 7.32-7.30 (m, 2H), 7.27-7.23 (m, 4H), 7.08-7.02 (m, 6H), 6.95-6.93 (m, 2H); ^{13}C NMR (100 MHz, $CDCl_3$) δ (ppm) 147.38, 147.03, 132.26, 129.39, 125.14, 124.42, 123.23, 114.76.

Compound 4: Compound **3** (775 mg, 2.40 mmol) was allowed to react with trimethylsilylacetylene (283 g, 2.88 mmol) for 12 hours under reflux conditions. The obtained residue was purified using column chromatography in hexane to yield compound, N, N-diphenyl-4-((trimethylsilyl)ethynyl)aniline. The resultant product (0.65 g, 1.92 mmol) was stirred with K_2CO_3 (0.8 g, 5.8 mmol) for 2 hours at room temperature**.** After the completion of the reaction, the organic layer was extracted with DCM, washed with brine, and dried over anhydrous Na_2SO_4. The crude was purified using column chromatography in hexane to yield compound **4.** Yellow solid (yield, 71 %). ^{1}H NMR (400 MHz, $CDCl_3$) δ (ppm): 7.34 (d, J=8.4 Hz, 2H),7.29-7.25 (m, 4H), 7.11-7.04 (m, 6H), 6.97 (d, J=8.4 Hz, 2H), 3.03 (s, 1H); ^{13}C NMR (100 MHz, CDCl3) δ (ppm): 148.30, 147.07, 133.09, 129.45, 125.07, 123.67, 122.08, 114.78, 83.96, 76.17.

Compound 5: In a 100 ml round bottom flask, $POCl_3$ (5.7 ml, 61.14 mmol) was slowly added to the DMF solution (7 ml, 97.76 mmol). Then the reaction mixture was allowed to stir for 1 hour at 0°C. Triphenylamine (3g, 12.22 mmol) was added to the reaction mixture and stirred for another 4 h at 70°C. The progress of the reaction was monitored by TLC. After completion, the mixture was poured into the ice-cold water and neutralized with NaOH solution. The crude was extracted with dichloromethane solution, and the combined organic layer was washed with brine solution and dried over anhydrous Na_2SO_4. The resultant organic layer was removed under reduced pressure. Column chromatography (v/v hexane-ethyl acetate: 9/1) was used to purify the desired product **5**. Yellow solid (yield 90 %). ^{1}H NMR (400 MHz, $CDCl_3$) δ (ppm) 9.89 (s, 2H), 7.78 (d, *J* = 8 Hz, 4H), 7.40 (t, *J* = 7.6 Hz, 2H), 7.29 –7.25 (t, *J* = 7.4 Hz, 1H), 7.19 (dd, *J* = 8.0, 4.4 Hz, 6H); ^{13}C NMR (100 MHz, $CDCl_3$) δ (ppm) 190.61, 152.02, 145.49, 131.35, 131.24, 130.18, 127.09, 126.29, 122.77.

Compound 6: Compound **5** (1.05 g, 3.49 mmol) was dissolved in 10 mL glacial acetic acid, and a mixture of KIO_3 (0.52 g, 2.44 mmol) and KI (0.96 g, 5.79 mmol) was added and refluxed at 110 °C for 4 hours. The obtained mixture was quenched with a saturated solution of sodium thiosulphate and the resultant precipitate was washed with water several times to give compound **6** in pure form. Yellow solid (yield 89 %). ^{1}H NMR (400 MHz, $CDCl_3$) δ (ppm) 9.90 (s, 2H), 7.79 (d, J = 8.0 Hz, 4H), 7.69 (d, J = 7.9 Hz, 2H), 7.19 (d, J = 8.4 Hz, 4H), 6.94 (d, J = 8.6 Hz, 2H). ^{13}C NMR (100 MHz, $CDCl_3$) δ(ppm) 190.56, 151.54, 145.38, 139.20, 131.64, 131.43, 128.49, 123.09, 90.07.

Compound 7: Compound **6** (1 g, 1.6 mmol) was allowed to react with trimethylsilylacetylene (0.29 g, 3 mmol) for 5 hours under reflux conditions to afford 4-((trimethylsilyl)ethynyl)-(N,N-di-(4-formylphenyl)aniline. The resultant product (0.81 g, 1.3 mmol) was stirred with K_2CO_3 (0.53 g, 3.8 mmol) for 2 hours as per the general procedure for trimethylsilyl deprotection to afford **7**. Yellow solid (yield 70 %). ^{1}H NMR (400 MHz, $CDCl_3$) δ (ppm) 9.91 (s, 2H), 7.80 (d, *J* = 8.4 Hz, 4H), 7.49 (d, *J* = 8.3 Hz, 2H), 7.20 (d, *J* = 8.4 Hz, 4H), 7.12 (d, *J* = 8.4 Hz, 2H), 3.13 (s, 1H). ^{13}C NMR (100 MHz, $CDCl_3$) δ (ppm) 190.57, 151.59, 145.94, 133.84, 131.76, 131.42, 126.02, 123.39, 119.31, 82.87, 78.04.

Compound 8: In a 100 ml round bottom flask triphenylamine (2 g, 8.15 mmol) was taken with DMF solution. Then, N-bromosuccinamide (2.93 g, 16.45) was slowly added to the reaction at 0˚ C. The reaction mixture was allowed to stir for 4 hours at 0˚ C. The progress of the reaction was monitored by TLC. The obtained mixture was quenched with water, and this resulted in a white precipitate. The crude was washed with water several times to give compound **8** as a product. White solid (yield 92 %). ^{1}H NMR (400 MHz, $CDCl_3$) δ(ppm) 7.38-7.30 (m, 4H), 7.29-7.23 (m, 2H), 7.10-7.02 (m, 3H), 6.97-6.90 (m, 4H); ^{13}C NMR (100 MHz, $CDCl_3$) δ(ppm) 146.53, 132.35, 129.56, 125.64, 125.42, 124.60, 123.75, 115.43.

Compound 9: A mixture of **8** (1 g, 2.5 mmol) in THF, $Pd(PPh_3)_4$ (0.14 g, 0.12 mmol), and 2M Na_2CO_3 was stirred under nitrogen for 20 mins. 4-*tert*-Butylphenylboronic acid (0.89 g, 5 mmol) was added to the reaction mixture and refluxed at 70 °C for 24 hours. After the completion of the reaction, the mixture was

poured over water and extracted with dichloromethane. The combined organic phase was dried over Na_2SO_4, and the solvent was removed under reduced pressure. The crude product was purified by column chromatography on silica gel (EtOAc: hexane) to afford **9.** White solid (yield, 77 %). ^{1}H NMR (400 MHz, $CDCl_3$) δ 7.52-7.43 (m, 12H), 7.30 (t, *J* = 7.3 Hz, 2H), 7.17-7.15 (m, 6H), 7.04 (t, *J* = 7.9 Hz, 1H), 1.36 (s, 18H). ^{13}C NMR (100 MHz, $CDCl_3$) δ 149.81, 147.63, 146.77, 137.80, 135.26, 129.34, 127.71, 126.36, 125.72, 124.58, 124.16, 123.02, 34.54, 31.41.

Compound, 10: A mixture of compound **9** (1 g, 1.96 mmol), KI (0.43 g, 2.61 mmol), KIO_3 (0.29 g, 1.35 mmol) was dissolved in glacial acetic acid and refluxed at 110 °C for 4 hours. After completion, the reaction mixture was quenched with saturated sodium thiosulphate solution and extracted with dichloromethane. The organic phase was removed under reduced pressure and purified by column chromatography (hexane) to afford compound **10.** Pale yellow solid (yield, 96 %). ^{1}H NMR (400 MHz, $CDCl_3$) δ 7.55-7.44 (m, 14H), 7.17 (d, *J* = 8.6 Hz, 4H), 6.93 (d, *J* = 8.8 Hz, 2H), 1.36 (s, 18H). ^{13}C NMR (100 MHz, $CDCl_3$) δ 145.26, 142.79, 141.41, 133.44, 132.88, 131.23, 123.12, 121.65, 121.00, 119.83, 80.47, 29.80, 26.66.

Compound 11: Compound **10** (1 g, 1.6 mmol) was refluxed with trimethylsilylacetylene (0.29 g, 3 mmol) for 5 hours to afford 4-((trimethylsilyl)ethynyl)-(N,N-di-(4-(*tert*-butyl(1,1'-biphenyl))aniline as pale yellow solid. The resultant product (0.81 g, 1.3 mmol) was stirred with K_2CO_3 (0.53 g, 3.8 mmol) for 2 hours as per the general procedure for trimethylsilyl deprotection to afford **11**. Yellow solid (yield, 66 %). ^{1}H NMR (400 MHz, $CDCl_3$) δ 7.54 – 7.49 (m, 8H), 7.46 (d, *J* = 8.4 Hz, 4H), 7.39 (d, *J* = 8.4 Hz, 2H), 7.19 (d, *J* = 8.4 Hz, 4H), 7.08 (d, *J* = 8.4 Hz, 2H), 3.04 (s, 1H), 1.36 (s, 18H). ^{13}C NMR (100 MHz, $CDCl_3$) δ 150.03, 148.13, 146.01, 137.61, 136.23, 133.16, 127.89, 126.42, 125.76, 125.04, 122.50, 115.02, 83.93, 34.55, 31.39.

Compounds 12a-d: To a solution of compound **1** (0.79 mmol, 1eq,), arylacetylene (compound **2/4/7/11**, (2 eq)) was slowly added to the reaction mixture under a nitrogen atmosphere as per the general procedure for Sonogashira reaction. After being stirred for 3 to 4 hours at room temperature, the reaction mixture was passed through celite pad. The crude was purified using column chromatography on silica gel (hexane: DCM) to afford compounds **12a-d** correspondingly**.**

Compound 12a:

Pale orange solid, yield: 70 % ^{1}H NMR (400 MHz, $CDCl_3$) δ 8.61 (m, 6H), 8.49 (m, 4H), 8.29 – 8.23 (m, 2H), 7.80 (m, 4H), 7.67 – 7.58 (m, 4H), 4.30 – 4.19 (m, 12H), 2.02 – 1.89 (m, 12H), 1.63 (m, 12H), 1.42 (m, 24H), 0.99 – 0.91 (m, 18H). ^{13}C NMR (100 MHz, $CDCl_3$) 143.79, 143.33, 142.79, 129.99, 129.92, 129.59, 128.77, 128.47, 128.29, 128.23, 127.83, 127.04, 125.87, 123.03, 122.83, 122.42, 121.91, 121.46, 91.32, 89.77, 73.26, 32.00, 30.14, 25.76, 22.36, 13.95. HRMS (ESI) (m/z): 1178.7438 [M]; Calculated: 1178.7438 [M].

Compound 12b:

Pale brown solid, yield: 65 % ^{1}H NMR (400 MHz, $CDCl_3$) δ 8.44 (d, *J* = 8.6 Hz, 2H), 8.28 (s, 2H), 7.61 (m, 2H), 7.37 (m, 4H), 7.20 (m, 8H), 7.08 – 7.04 (m, 8H), 7.02 – 6.95 (m, 8H), 4.14 (t, *J* = 6.7 Hz, 4H), 1.84 (m, 4H), 1.50 (s, 4H), 1.35 – 1.24 (m, 8H), 0.85 (m, 6H). ^{13}C NMR (100 MHz, $CDCl_3$) δ 147.93, 147.20, 143.25, 132.57, 129.72, 129.43, 128.57, 127.66, 127.52, 125.53, 125.02, 123.48, 123.44, 122.88, 122.32, 122.01, 116.06, 90.51, 89.29, 73.70, 31.73, 30.42, 25.90, 22.74, 14.06. HRMS (ESI) (m/z): 912.4548 [M]; Calculated: 912.4548 [M].

Compound 12c:

Yellow solid, yield: 60 % ^{1}H NMR (400 MHz, $CDCl_3$) δ 8.53 (d, *J* = 8.7 Hz, 2H), 8.37 (s, 2H), 7.70 (d, *J* = 8.5 Hz, 2H), 7.55 – 7.45 (m, 28H), 7.25 – 7.19 (m, 8H), 7.14 (d, *J* = 8.7 Hz, 4H), 4.22 (t, *J* = 6.7 Hz, 4H), 1.98 –

1.89 (m, 4H), 1.40 – 1.32 (m, 44H), 1.11 (s, 4H), 0.94 (m, 6H). ^{13}C NMR (100 MHz, $CDCl_3$) δ 143.79, 143.33, 142.79, 129.99, 129.92, 129.59, 128.77, 128.47, 128.29, 128.23, 127.83, 127.04, 125.87, 123.03, 122.83, 122.42, 121.91, 121.46, 91.32, 89.77, 73.26, 32.00, 30.14, 25.76, 22.36, 13.95. HRMS (ESI) (m/z) 1141.8351 [M]; Calculated: 1141.8350 [M].

Compound 12d:

Orange solid, yield: 60 % ^{1}H NMR (400 MHz, $CDCl_3$) δ 9.93 (s, 4H), 8.58 (d, J = 8.4 Hz, 2H), 8.40 (s, 2H), 7.83 (d, J = 8 Hz, 8H), 7.73 (m,2H), 7.62 (m, 4H), 7.26-7.23 (m, 8H), 7.19-7.17 (m, 4H), 4.25-4.22 (t, J = 6.8 Hz, 4H), 1.98-1.91 (m, 4H), 1.43-1.39 (m, 8H), 1.15 – 1.07 (m, 4H), 0.97-0.90 (m, 6H). ^{13}C NMR (100 MHz, CDCl3) δ 190.31, 151.93, 145.35, 142.51, 133.81, 131.61, 131.33, 129.41, 128.21, 126.02, 123.81, 120.98, 120.71, 90.40, 89.13, 73.56, 37.93, 31.43, 25.48, 22.71, 13.31. HRMS (ESI) (m/z) 1024.2474, Calculated: 1024.4510 [M].

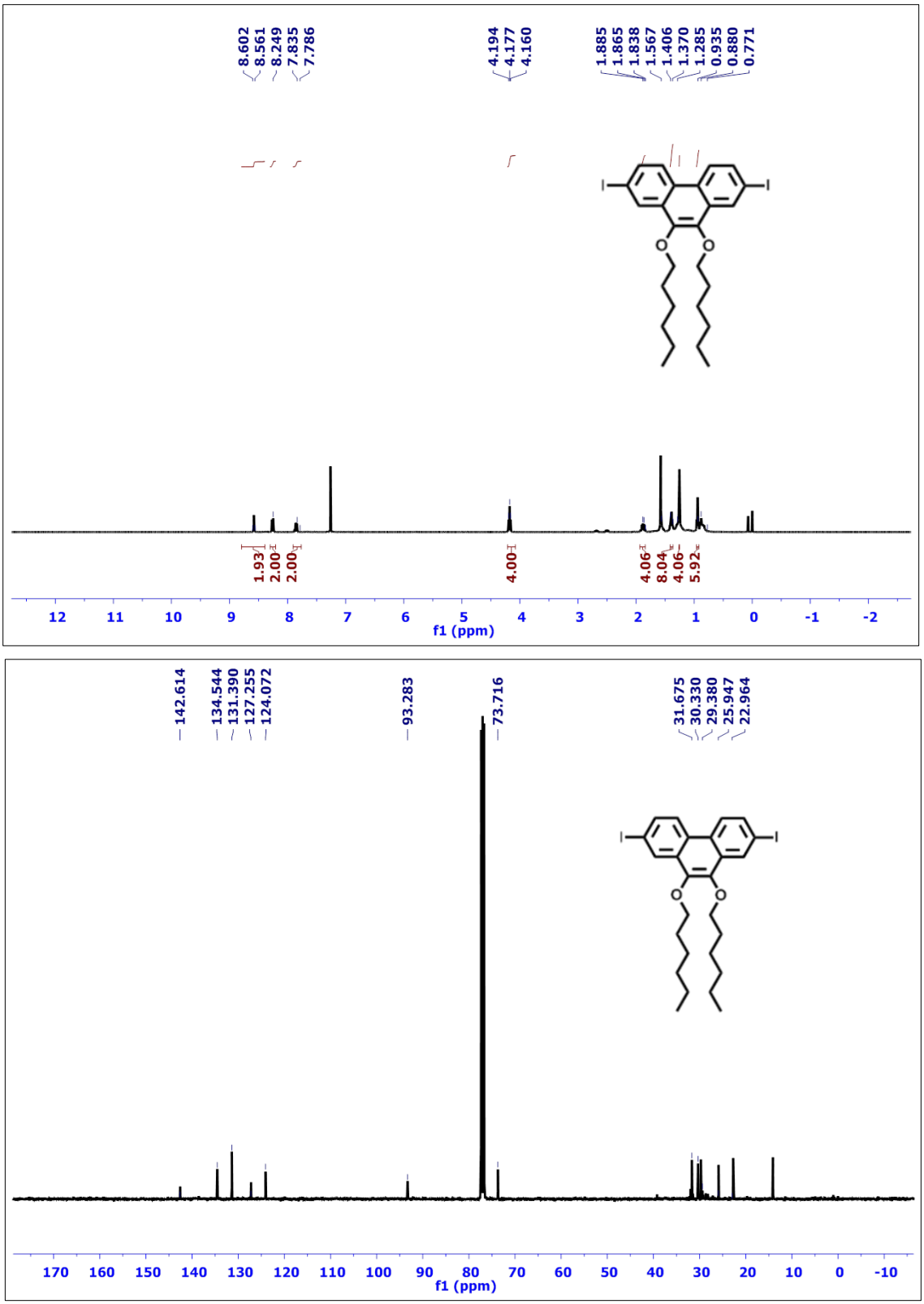

Figure S1: ^{1}H and ^{13}C NMR spectra of compound 1a

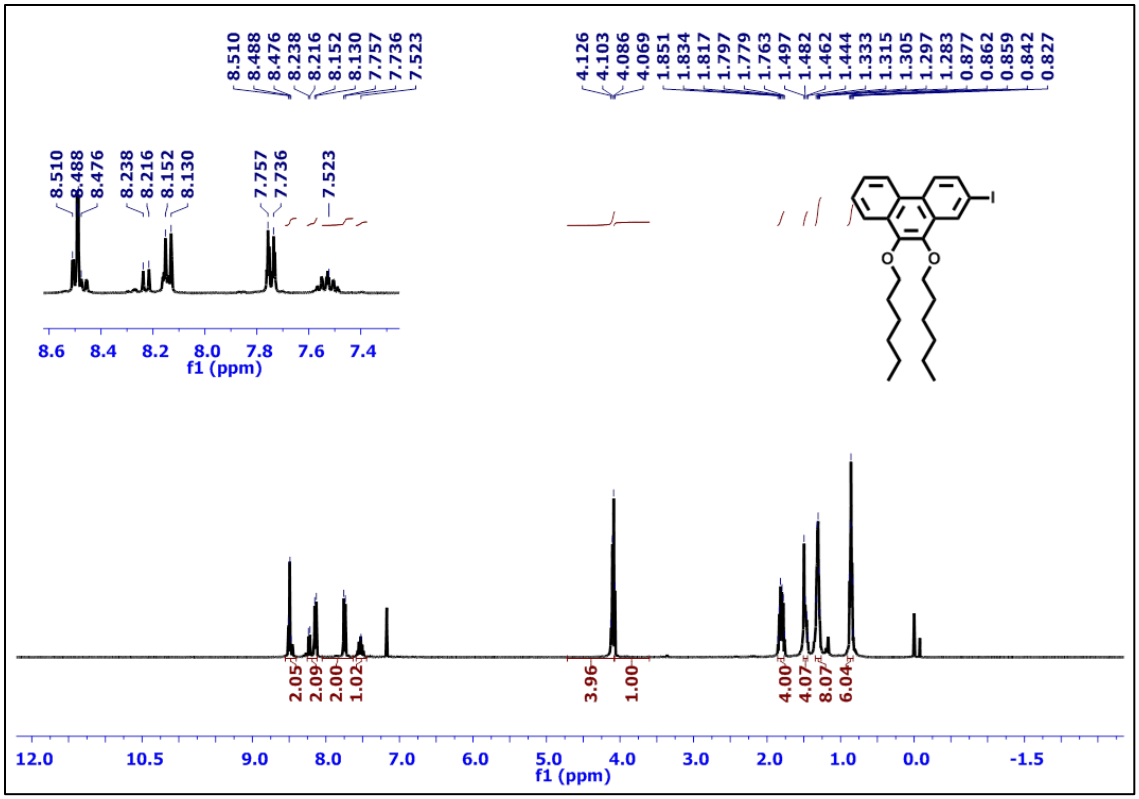

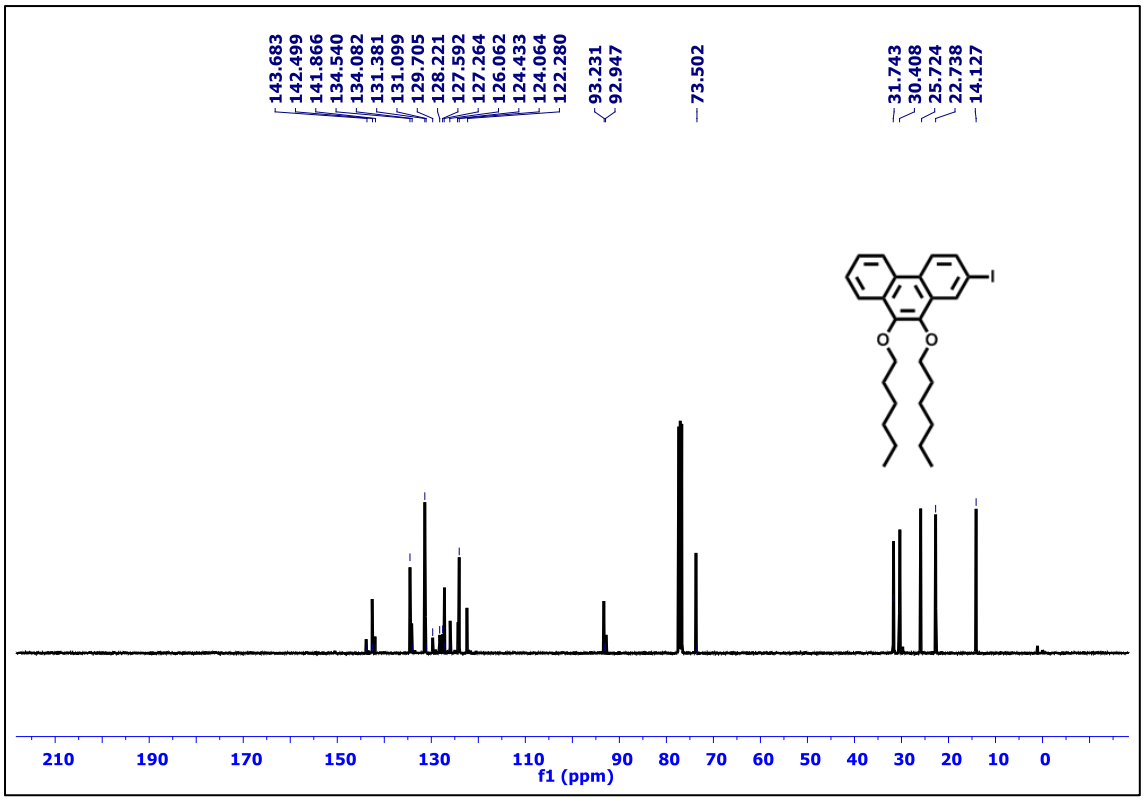

Figure S2: ^{1}H and ^{13}C NMR spectra of compound 1b

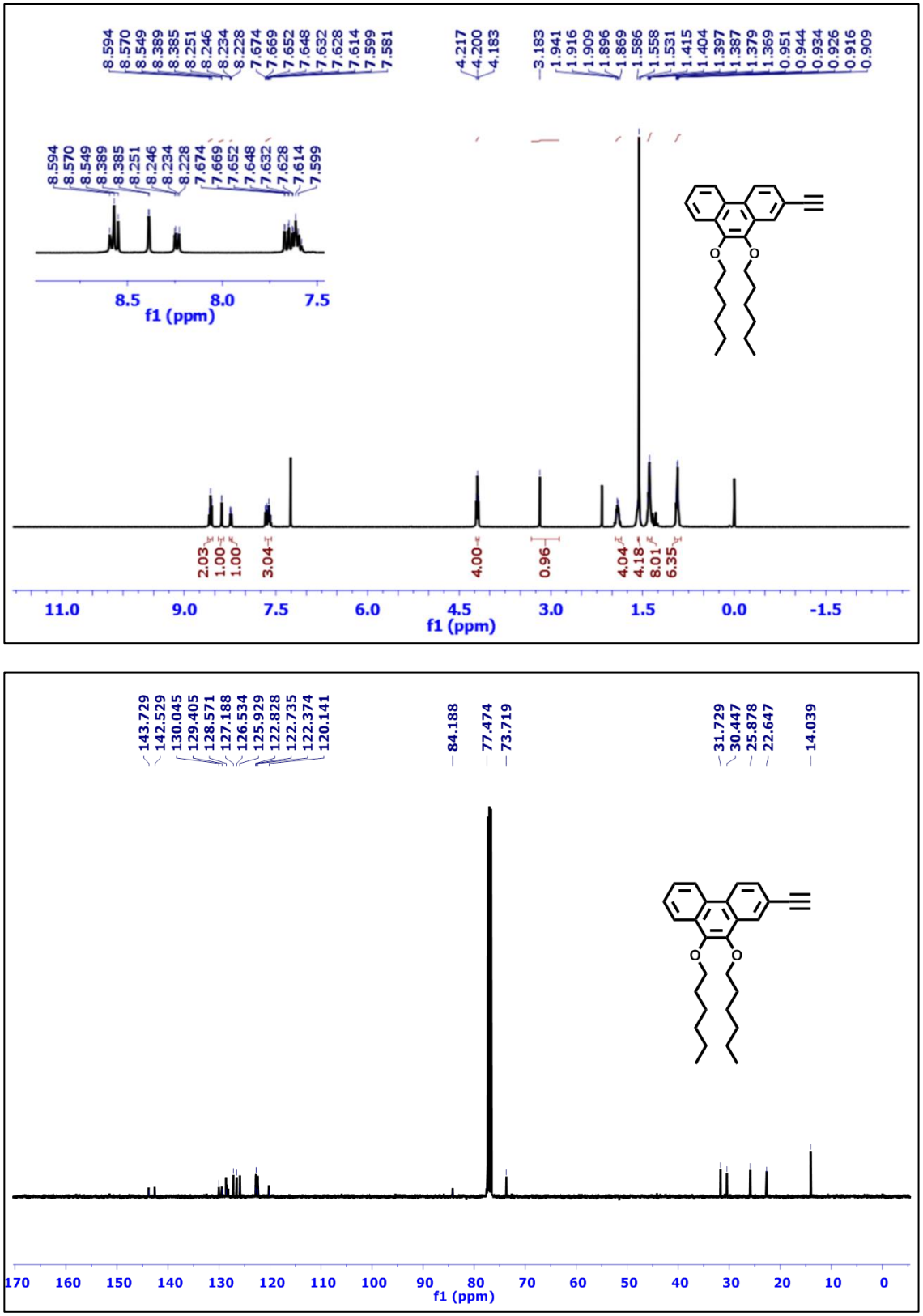

Figure S3: ^{1}H and ^{13}C NMR spectra of compound 2

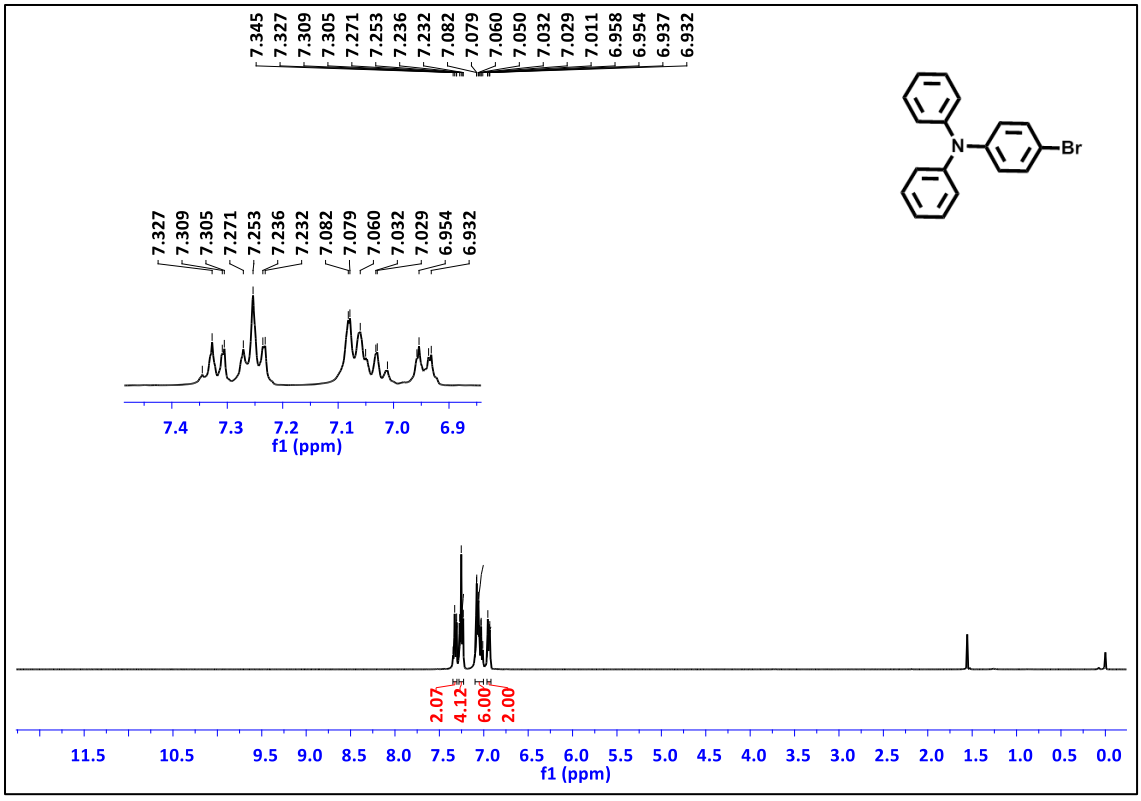

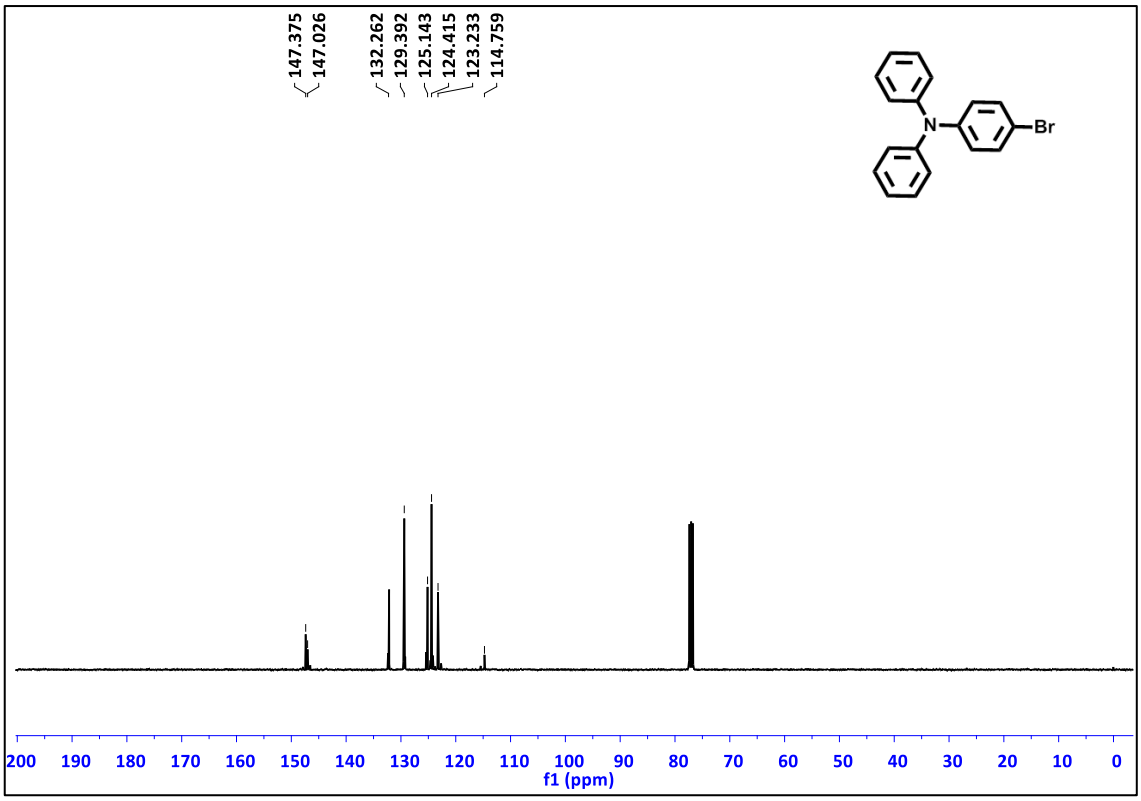

Figure S4: ^{1}H and ^{13}C NMR spectra of compound 3

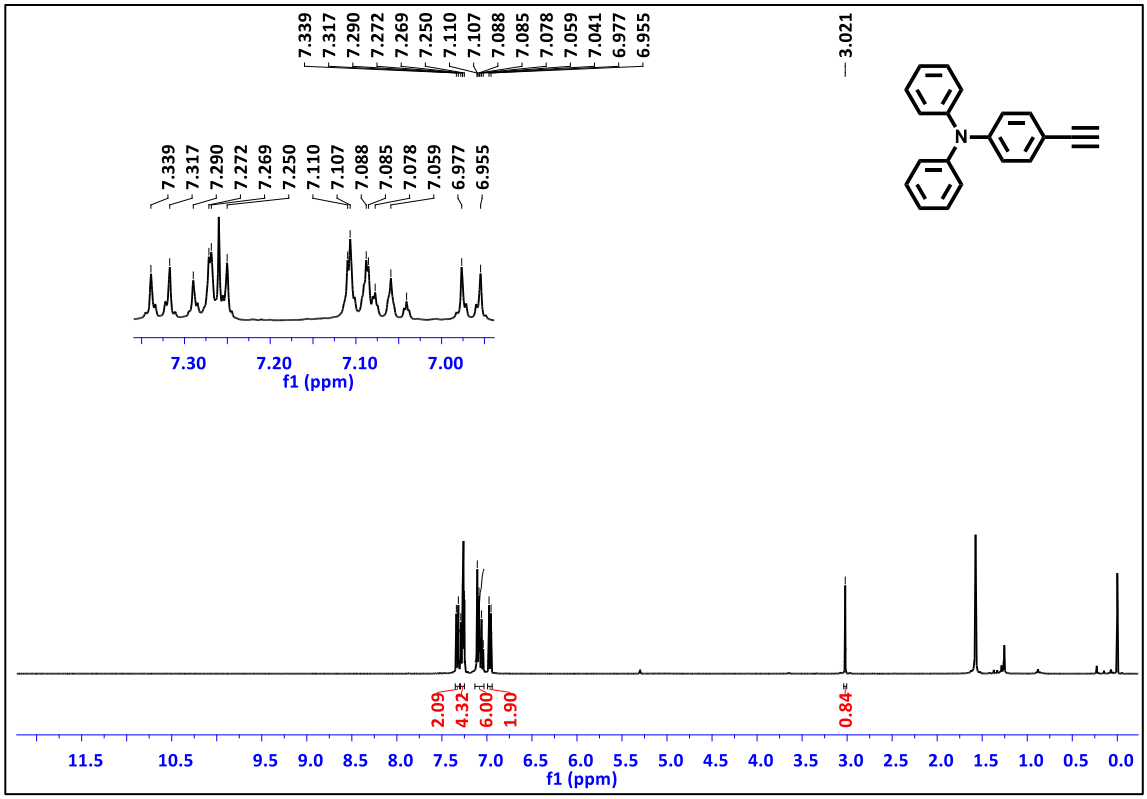

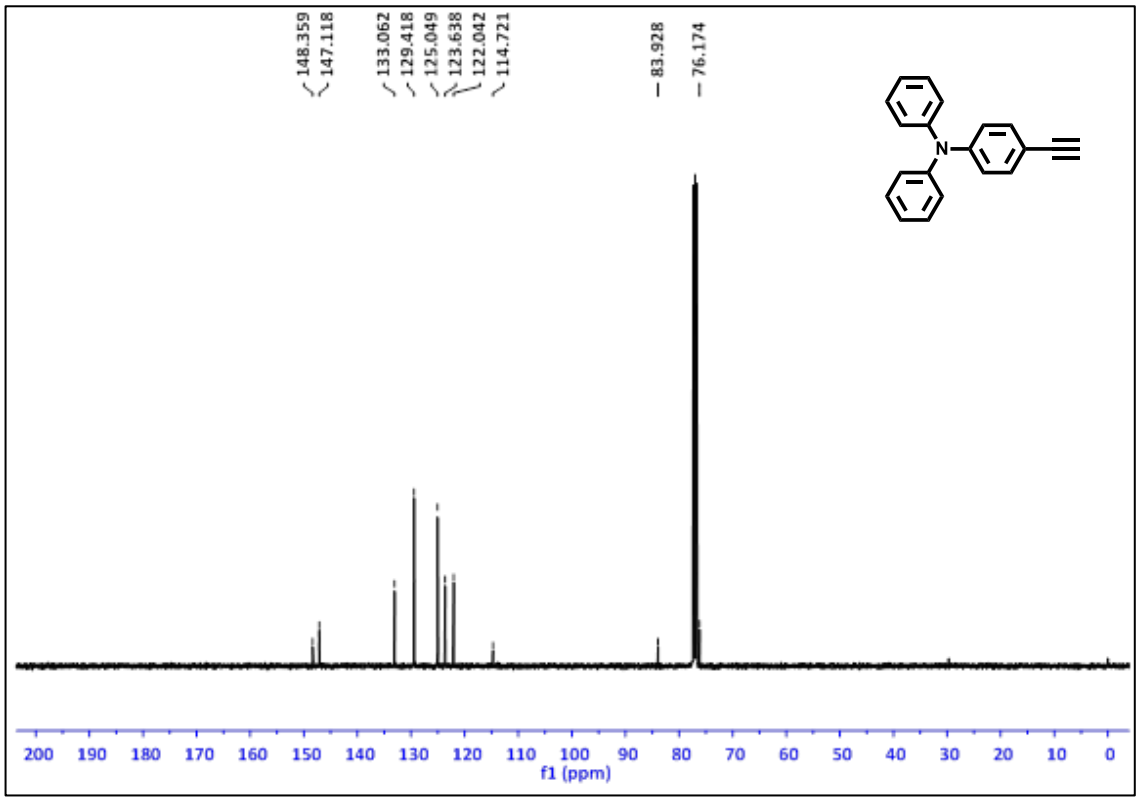

Figure S5: ^{1}H and ^{13}C NMR spectra of compound 4

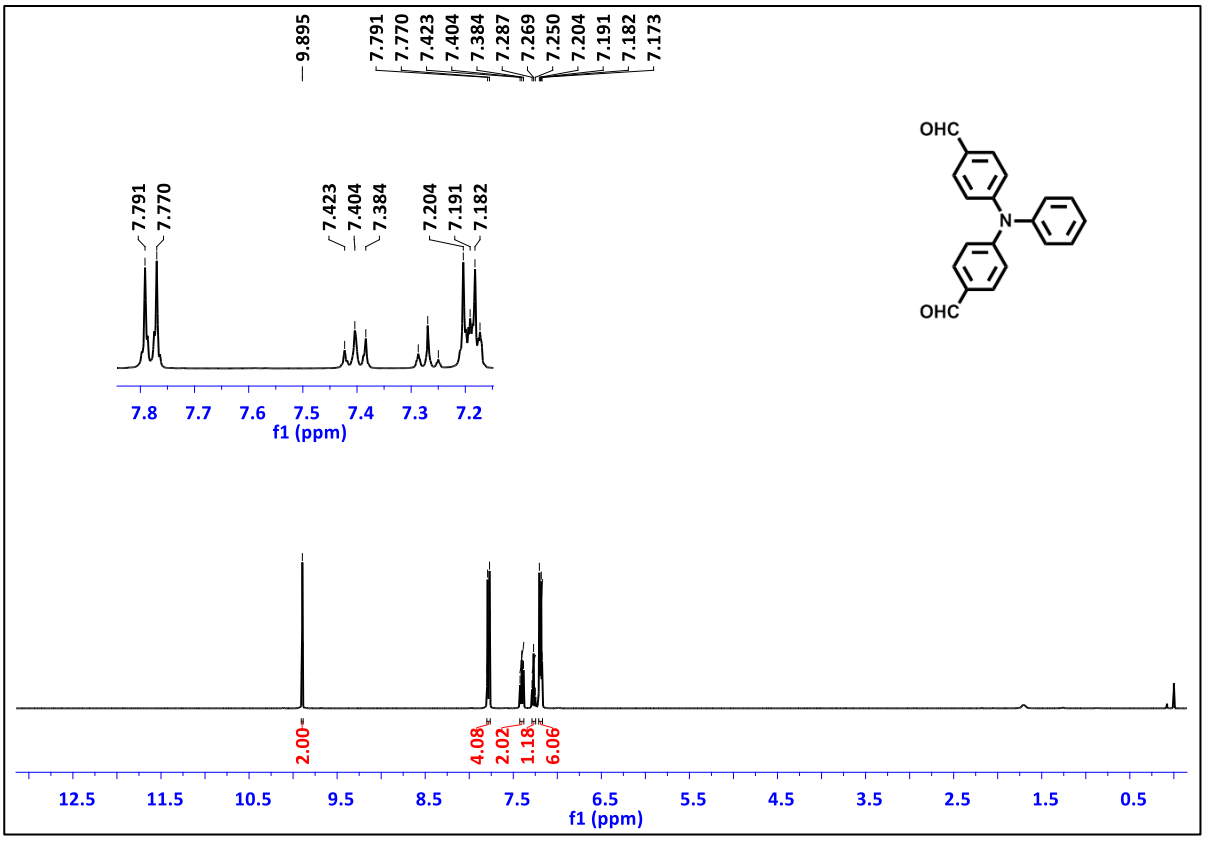

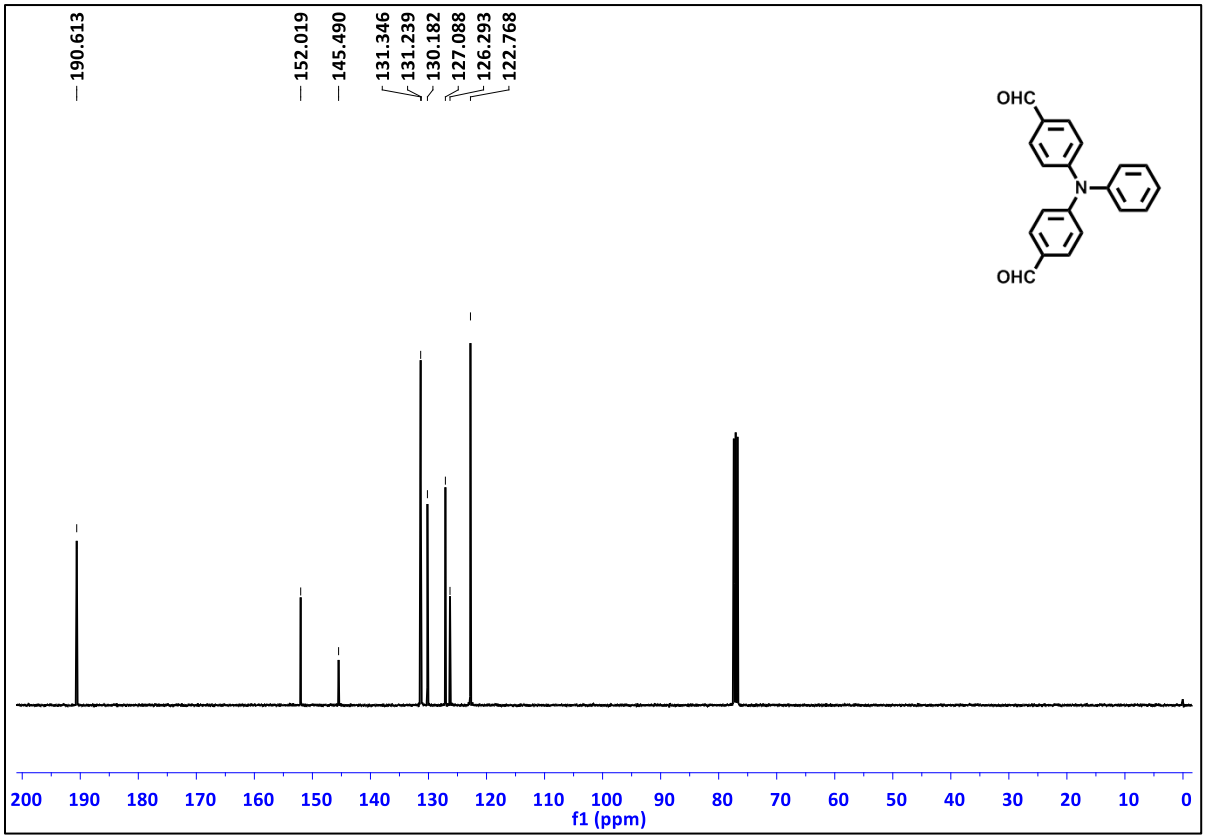

Figure S6: ^{1}H and ^{13}C NMR spectra of compound 5

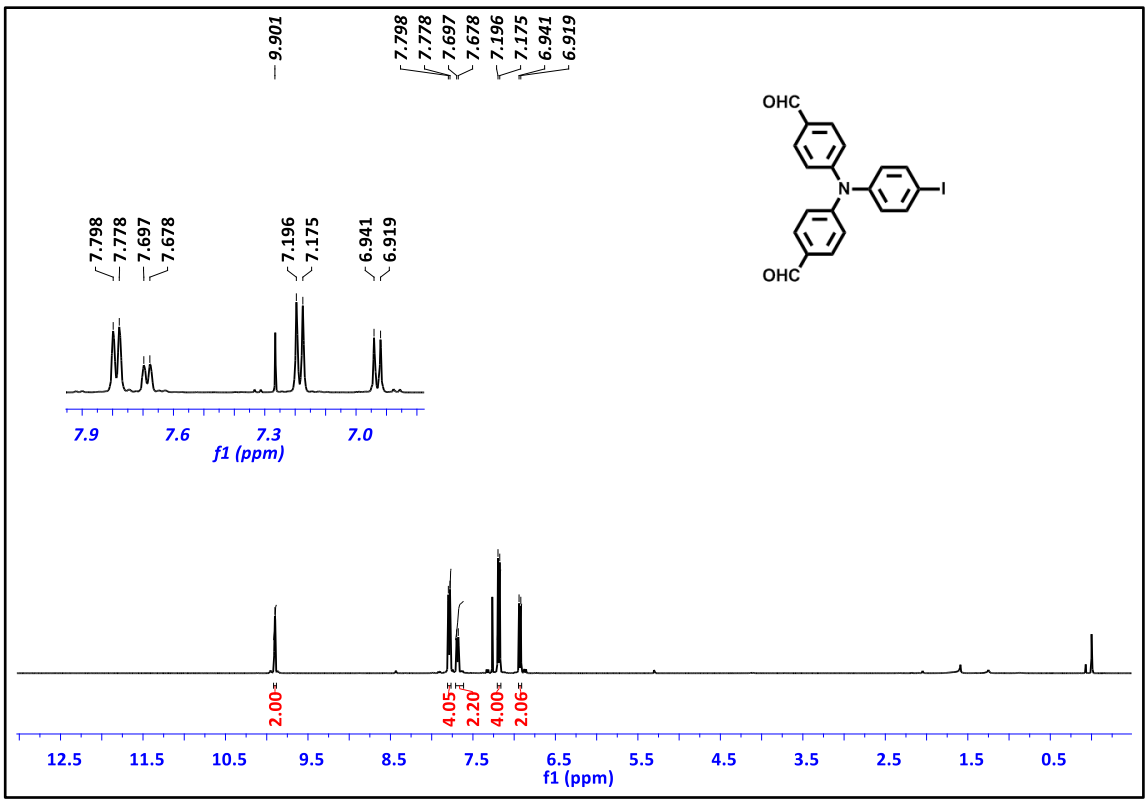

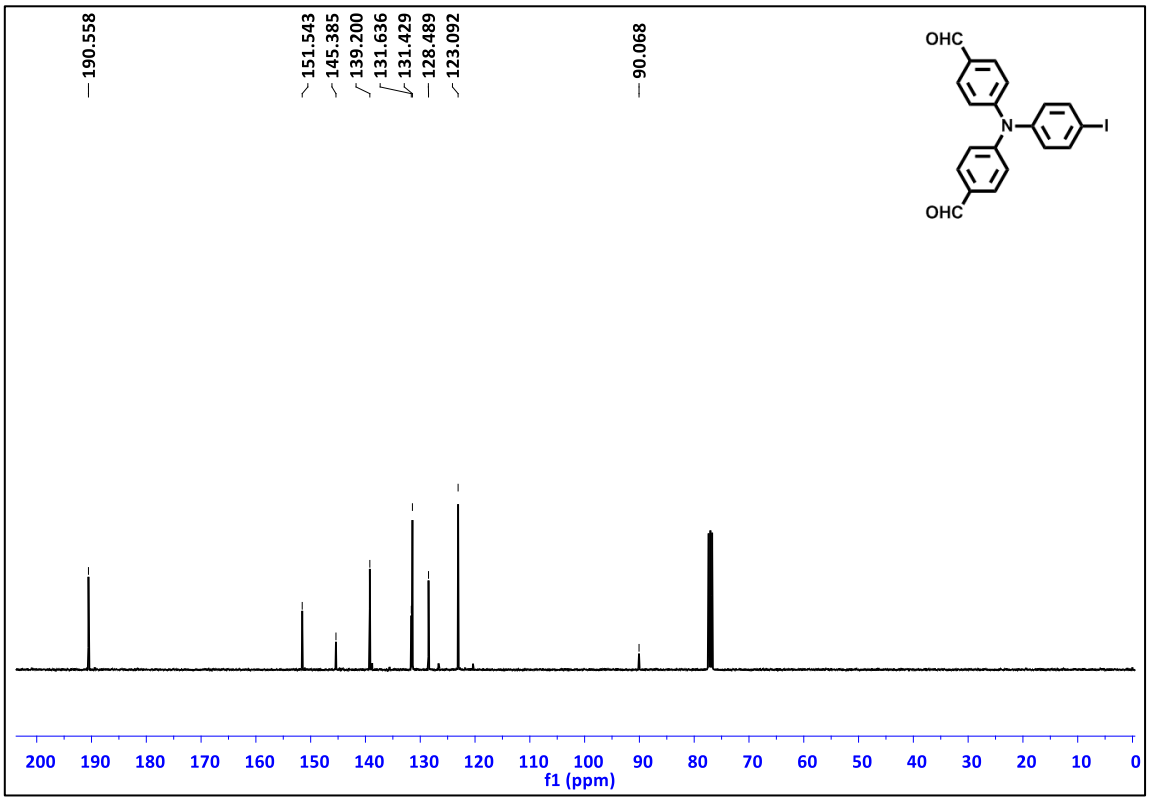

Figure S7: ^{1}H and ^{13}C NMR spectra of compound 6

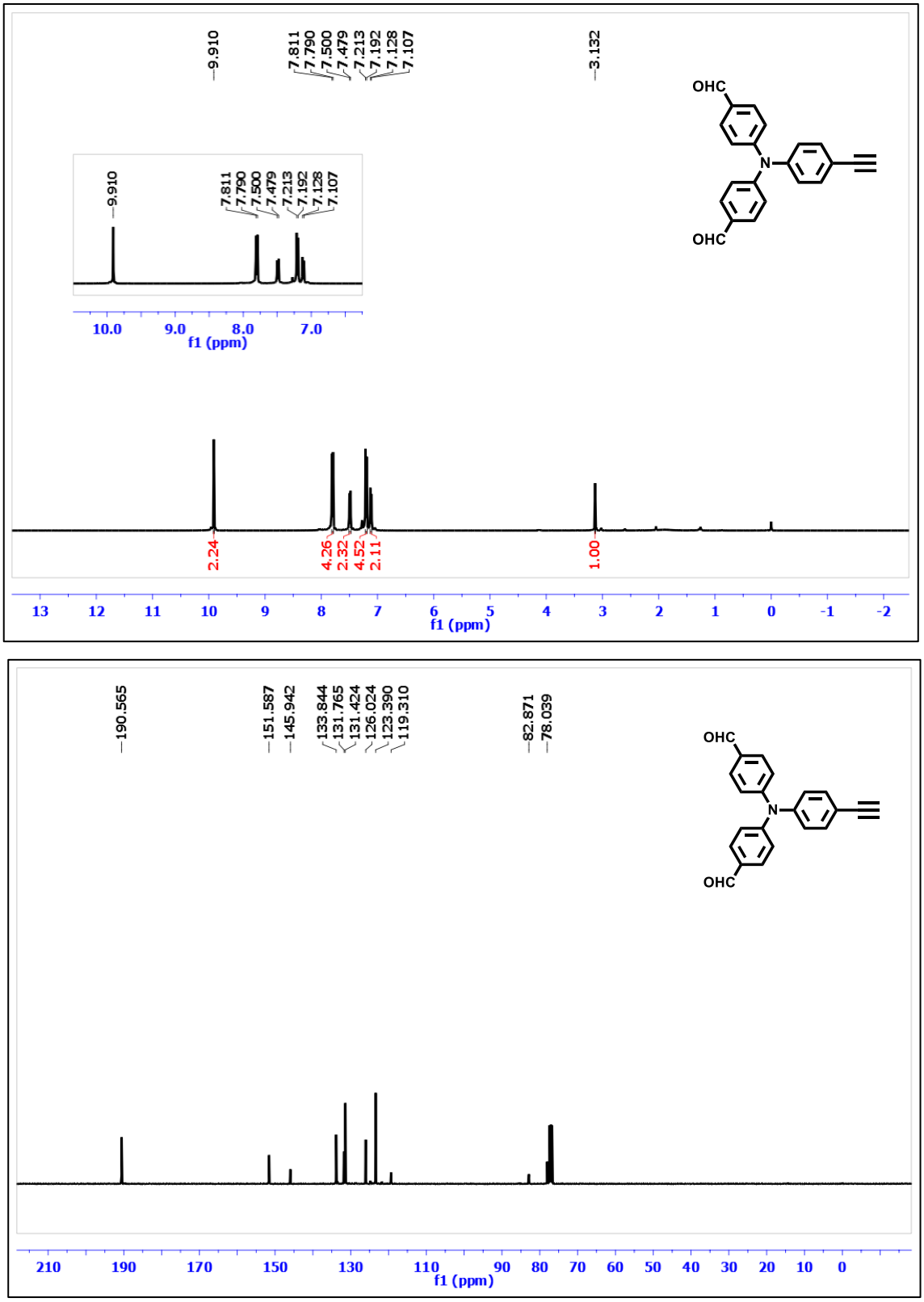

Figure S8: ^{1}H and ^{13}C NMR spectra of compound 7

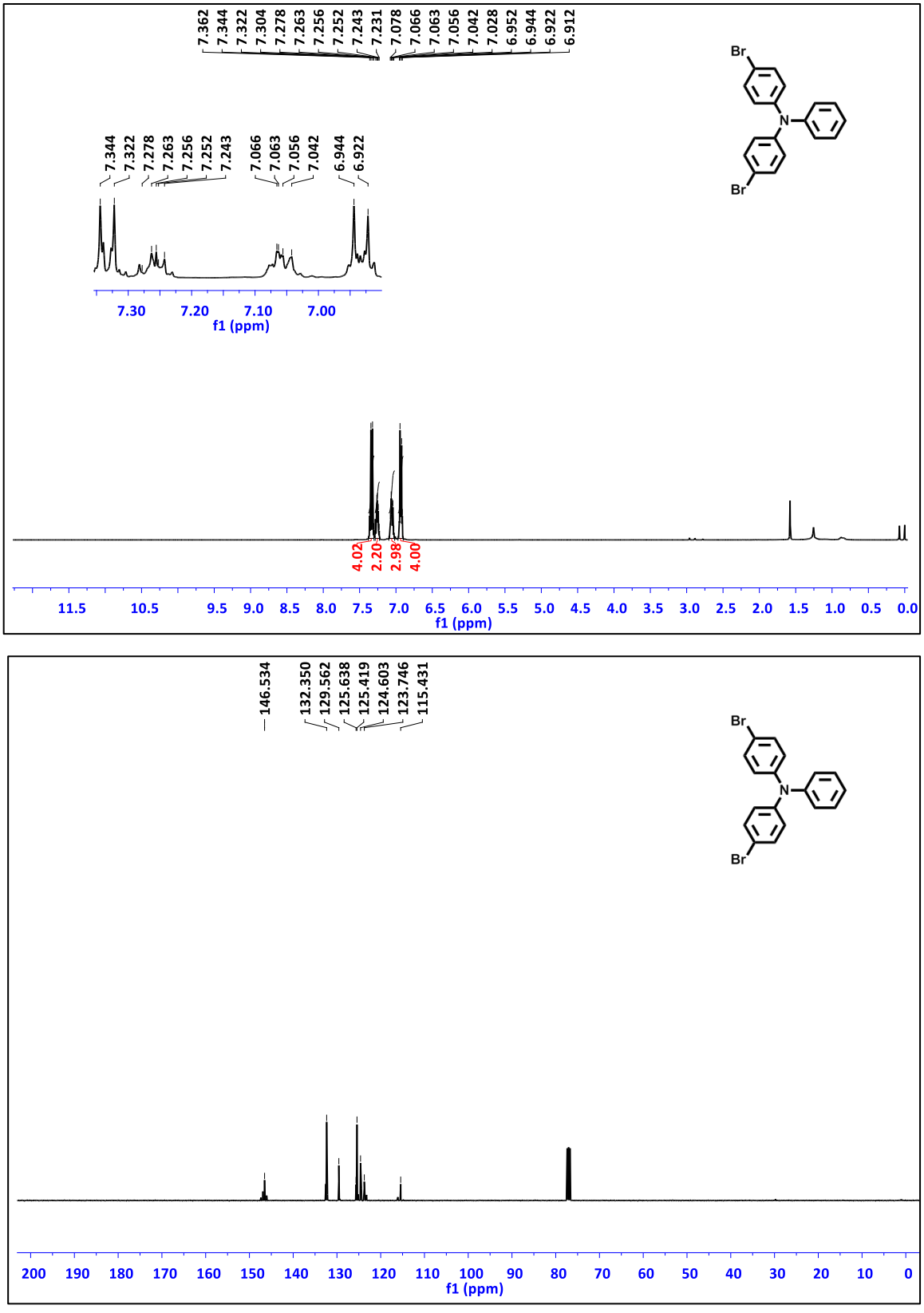

Figure S9: ^{1}H and ^{13}C NMR spectra of compound 8

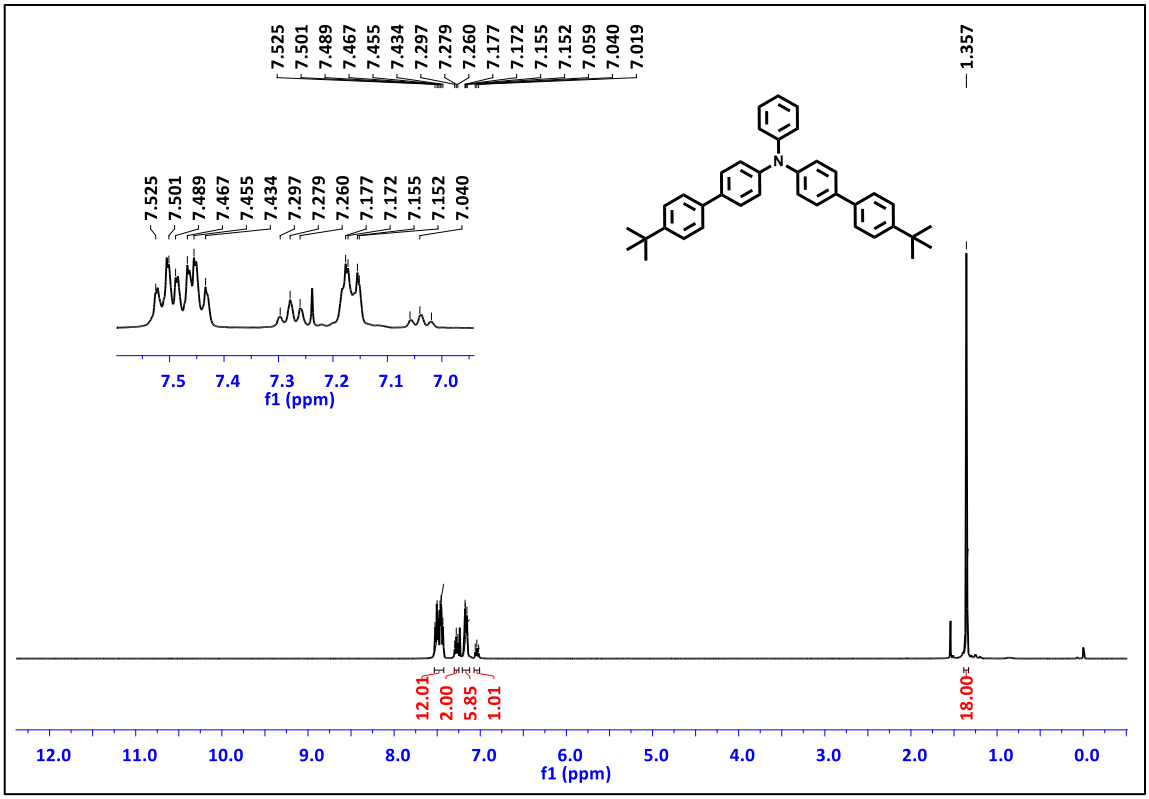

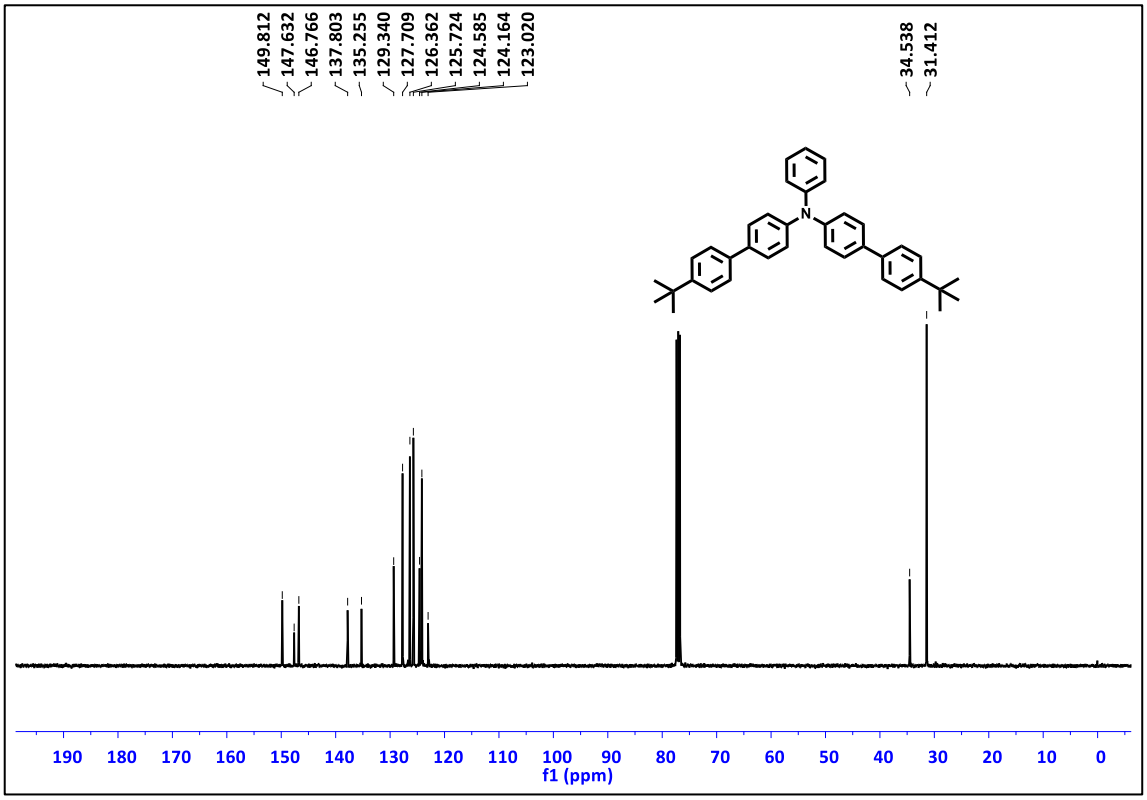

Figure S10: ^{1}H and ^{13}C NMR spectra of compound 9

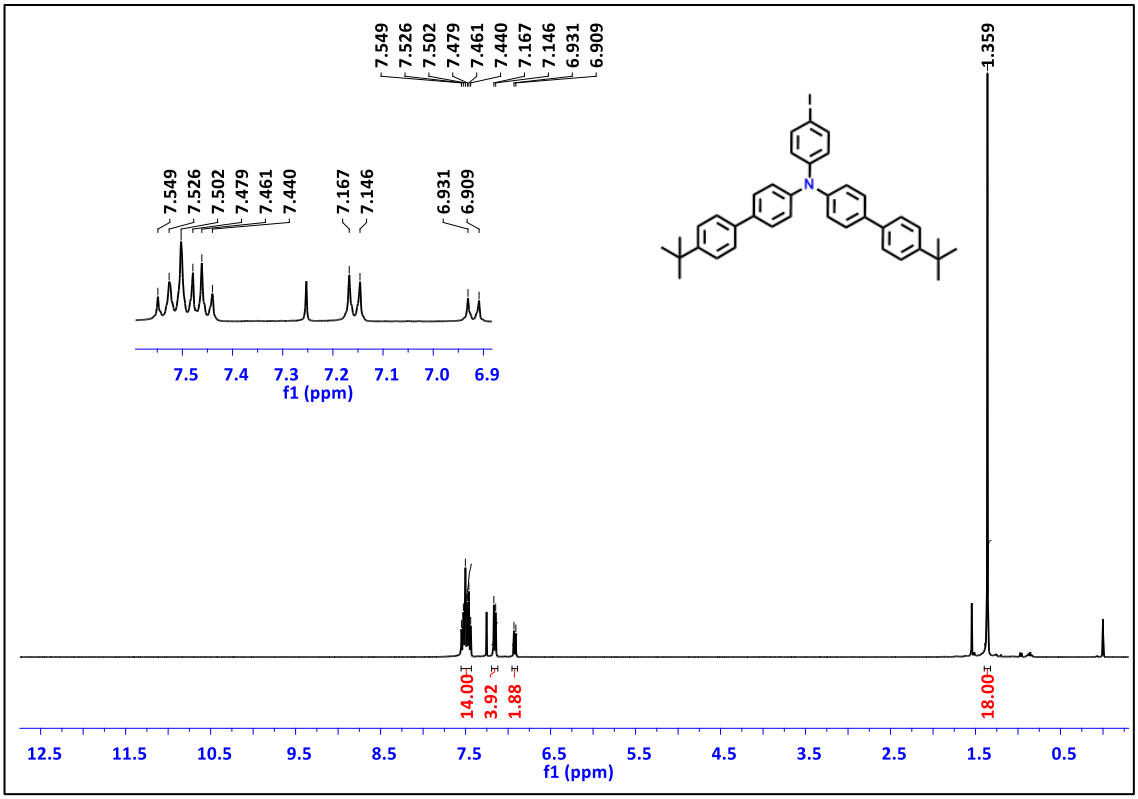

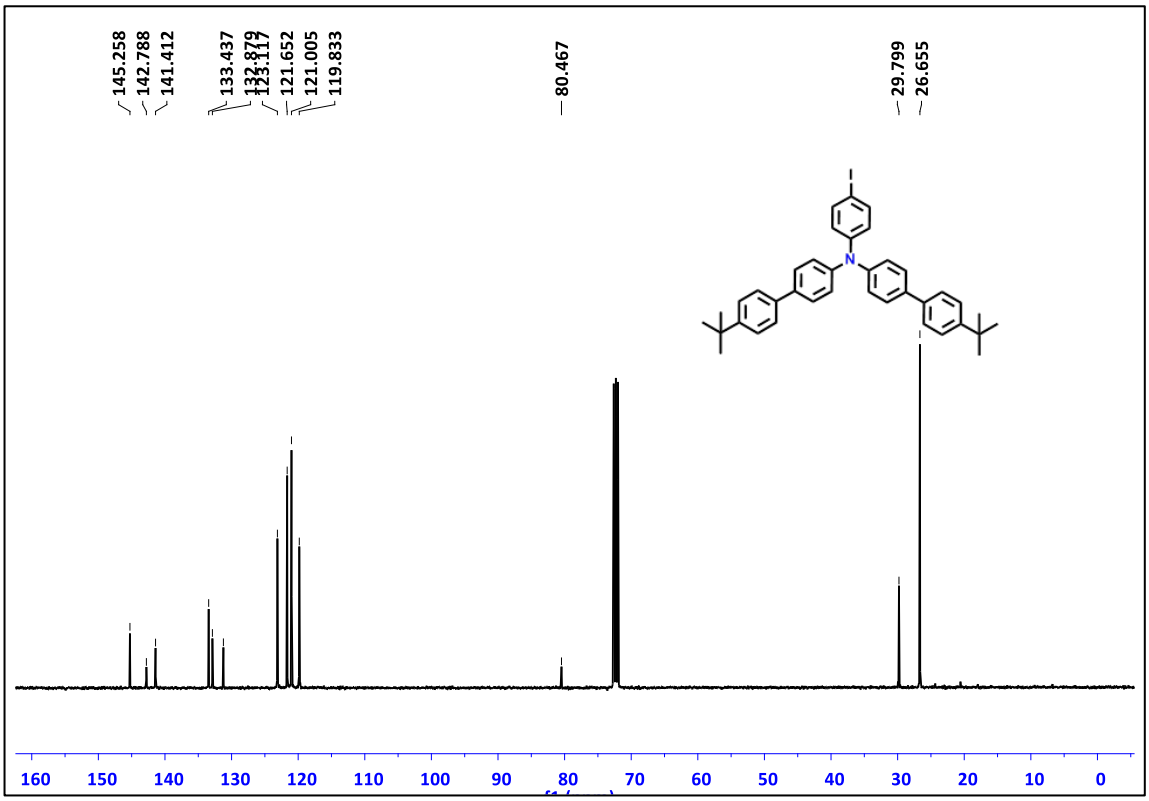

Figure S11: ^{1}H and ^{13}C NMR spectra of compound 10

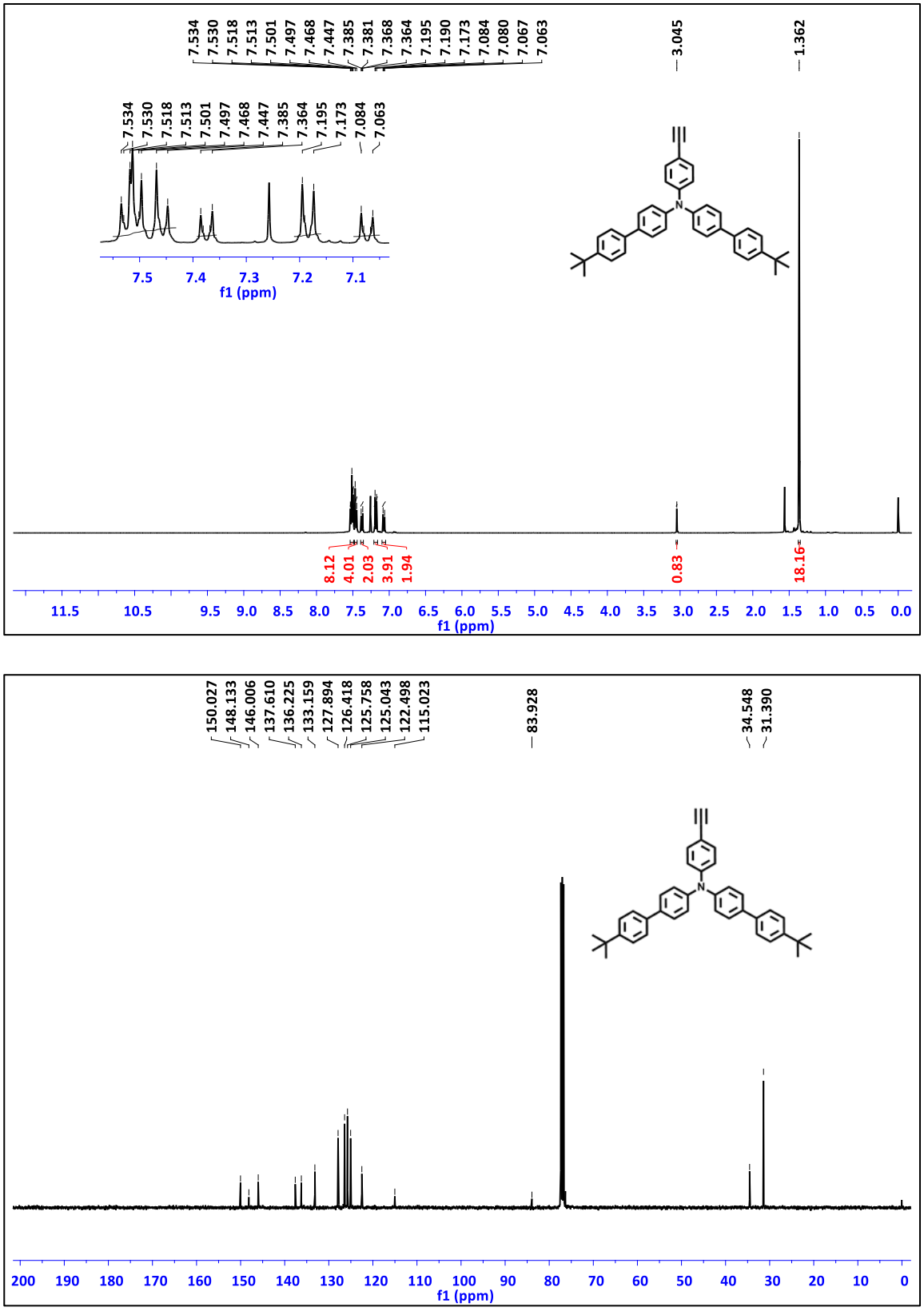

Figure S12: ^{1}H and ^{13}C NMR spectra of compound 11

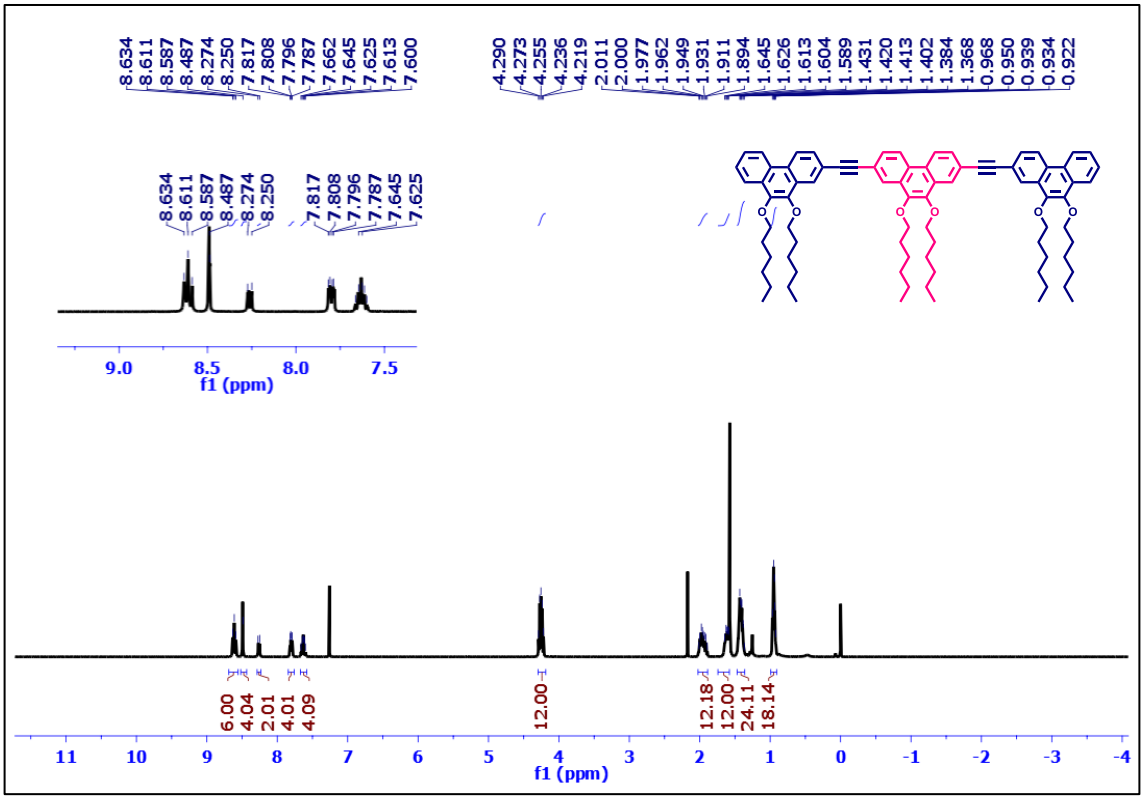

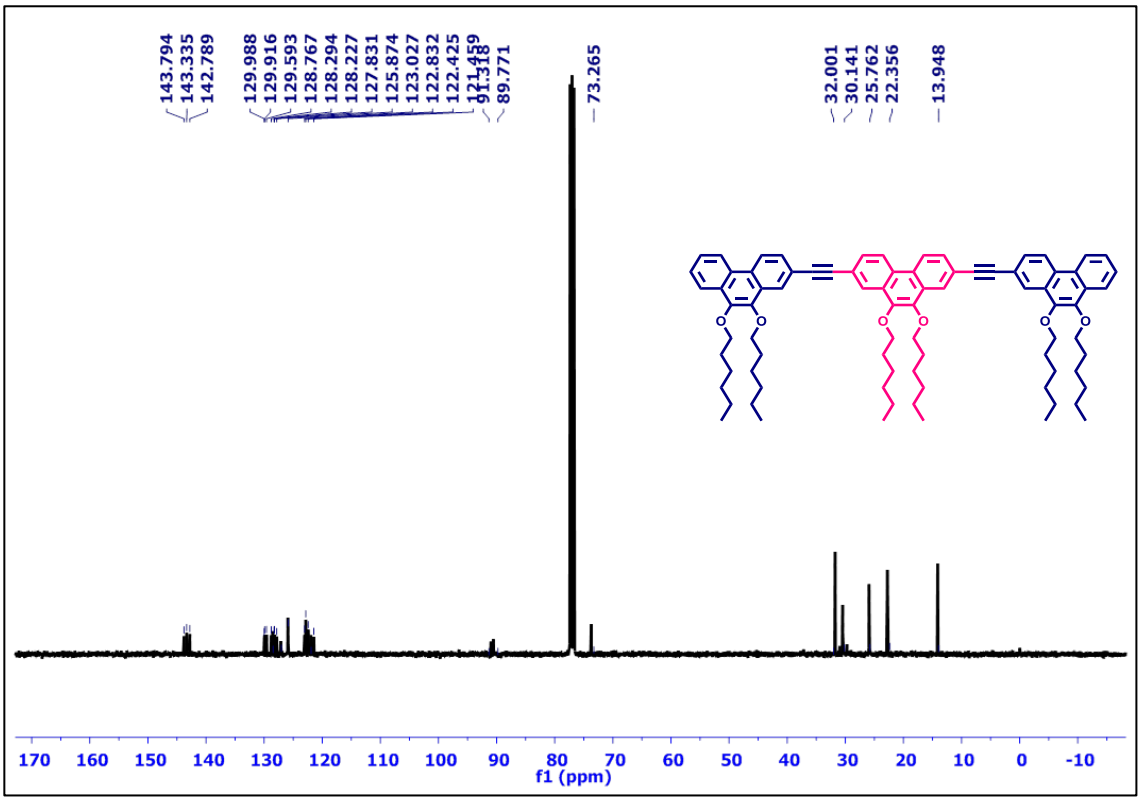

Figure S13: ^{1}H and ^{13}C NMR spectra of compound 12a

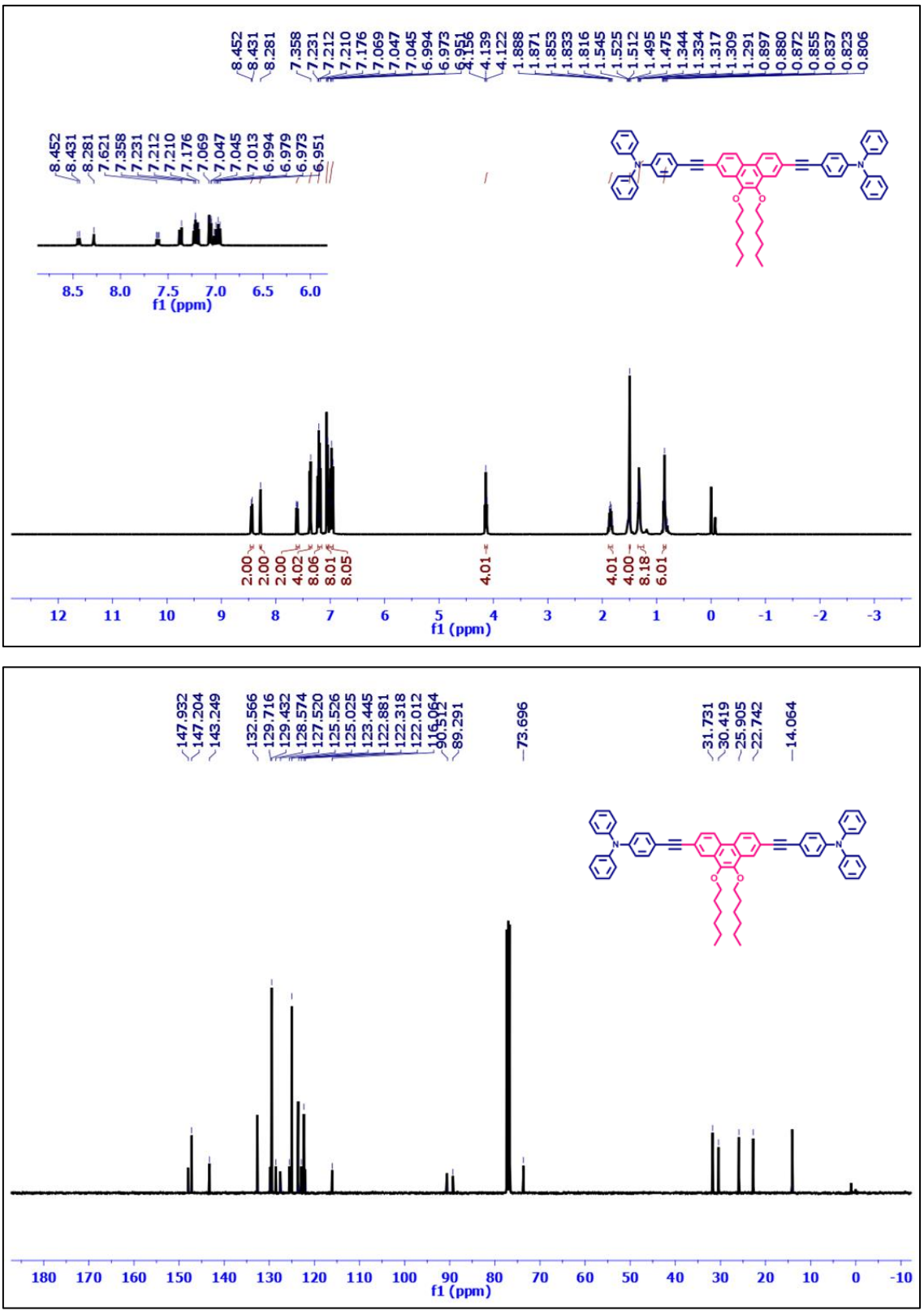

Figure S14: ^{1}H and ^{13}C NMR spectra of compound 12b

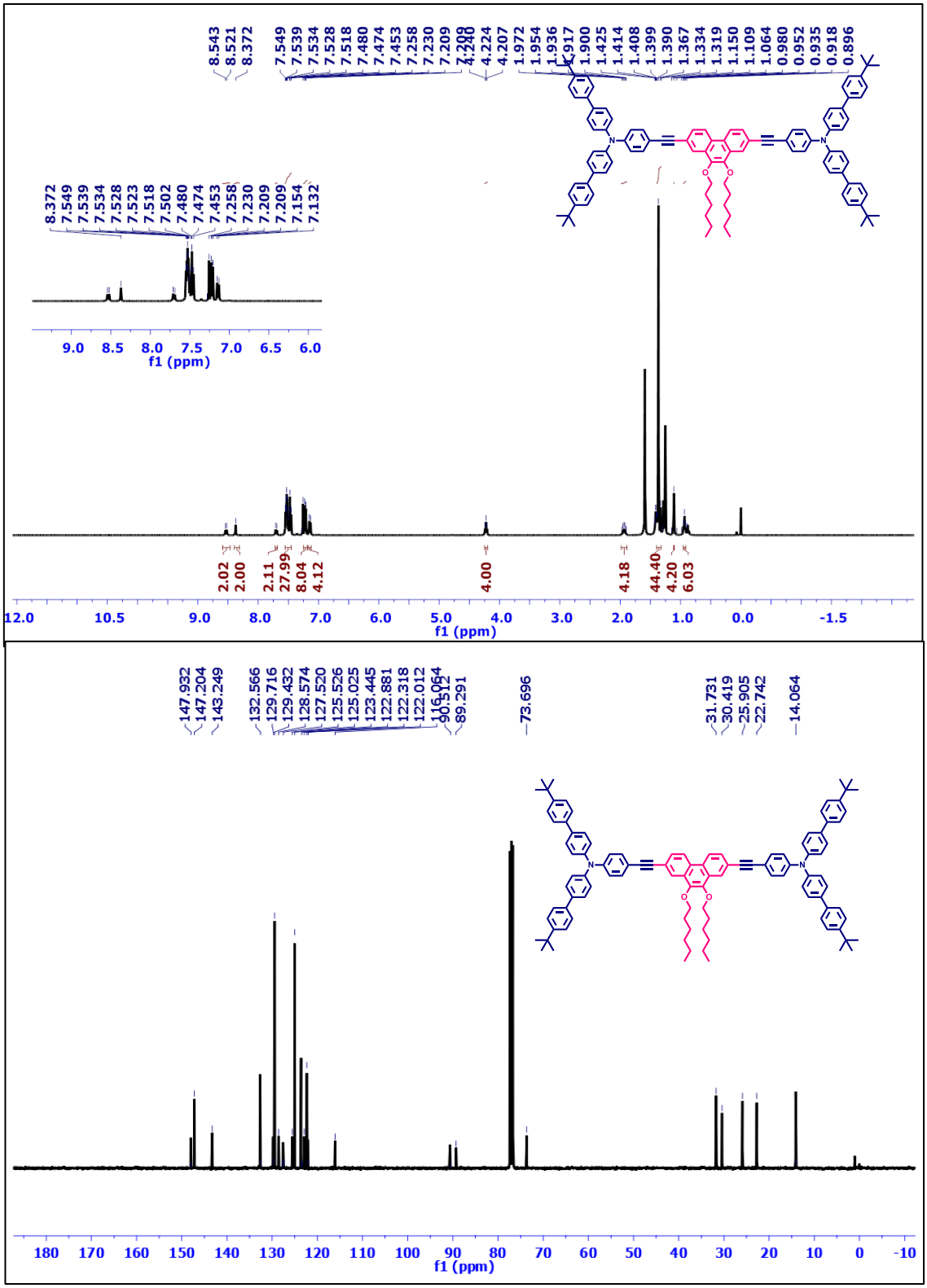

Figure S15: ^{1}H and ^{13}C NMR spectra of compound 12c

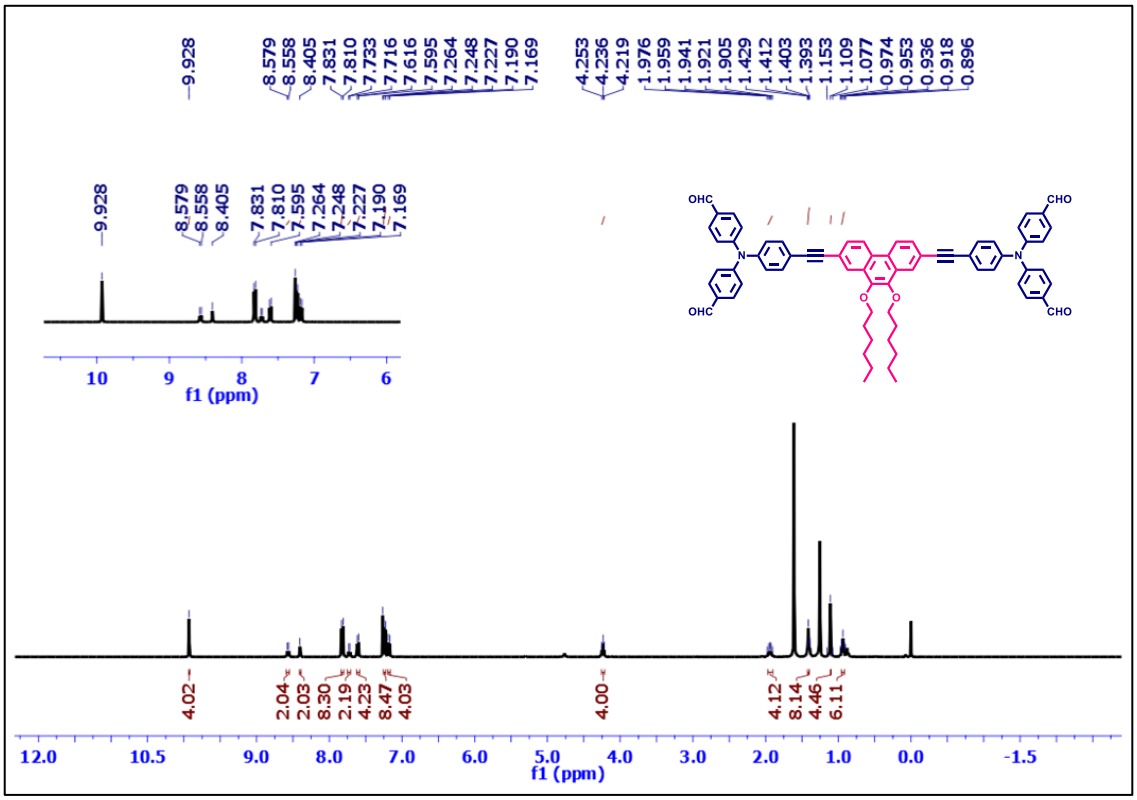

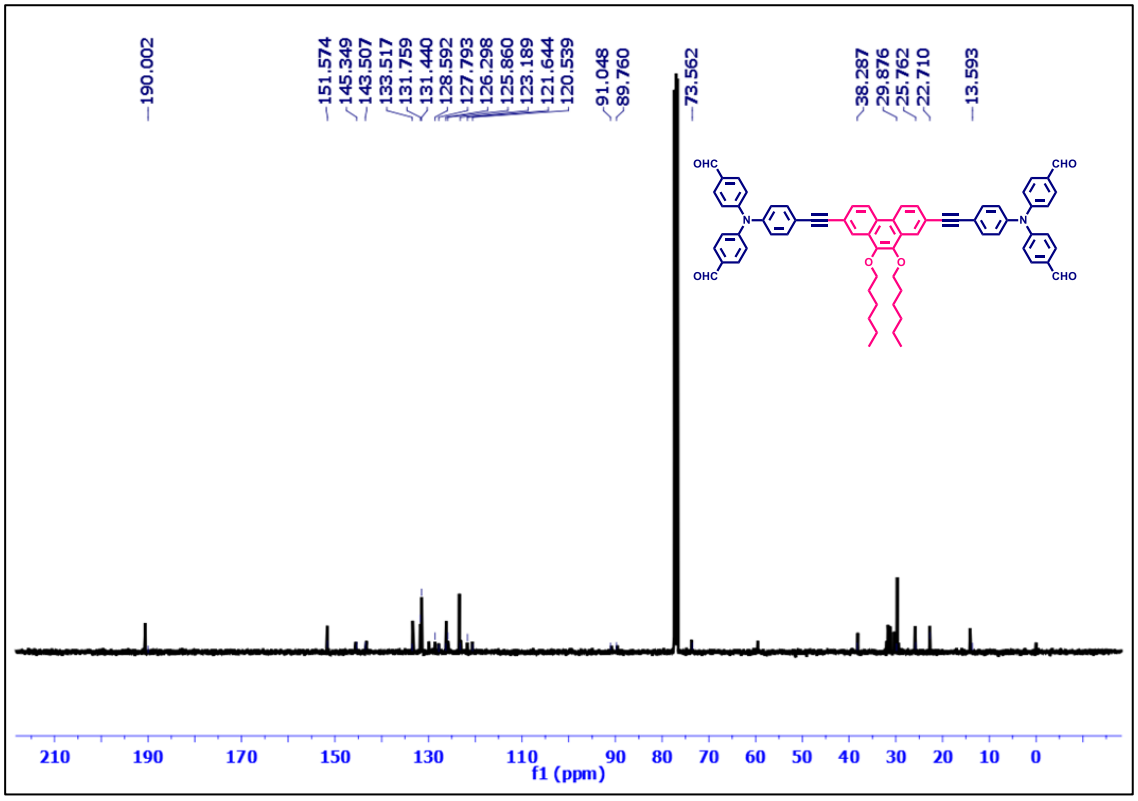

Figure S16: ^{1}H and ^{13}C NMR spectra of compound 12d

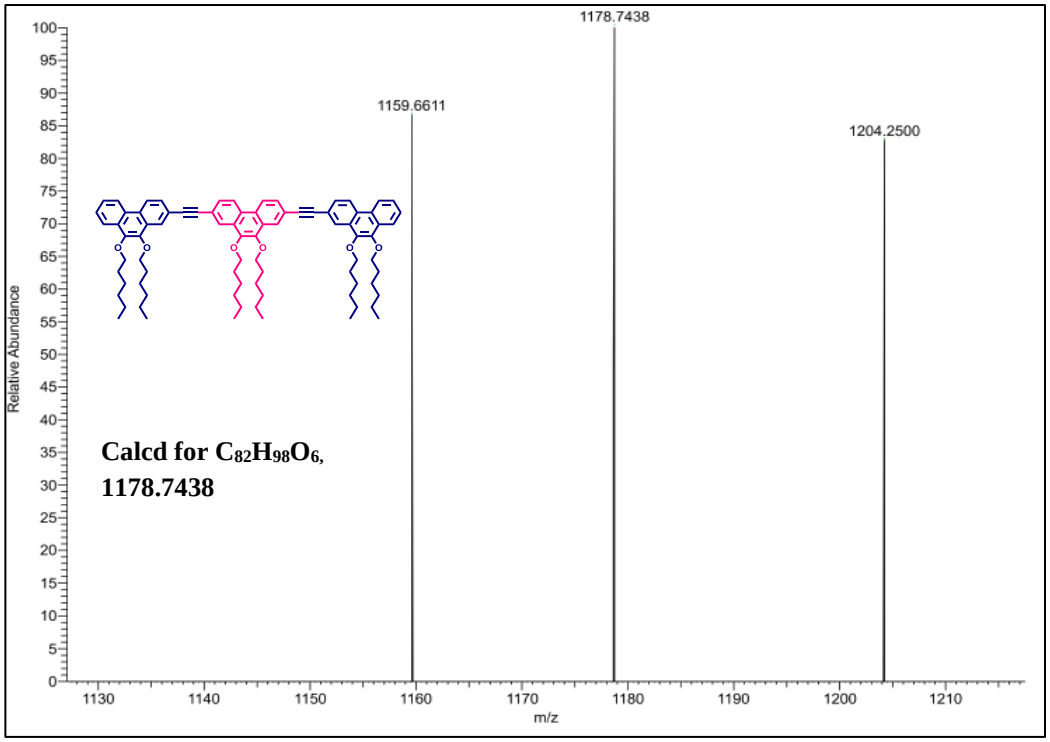

Figure S17: HRMS spectrum of compound 12a

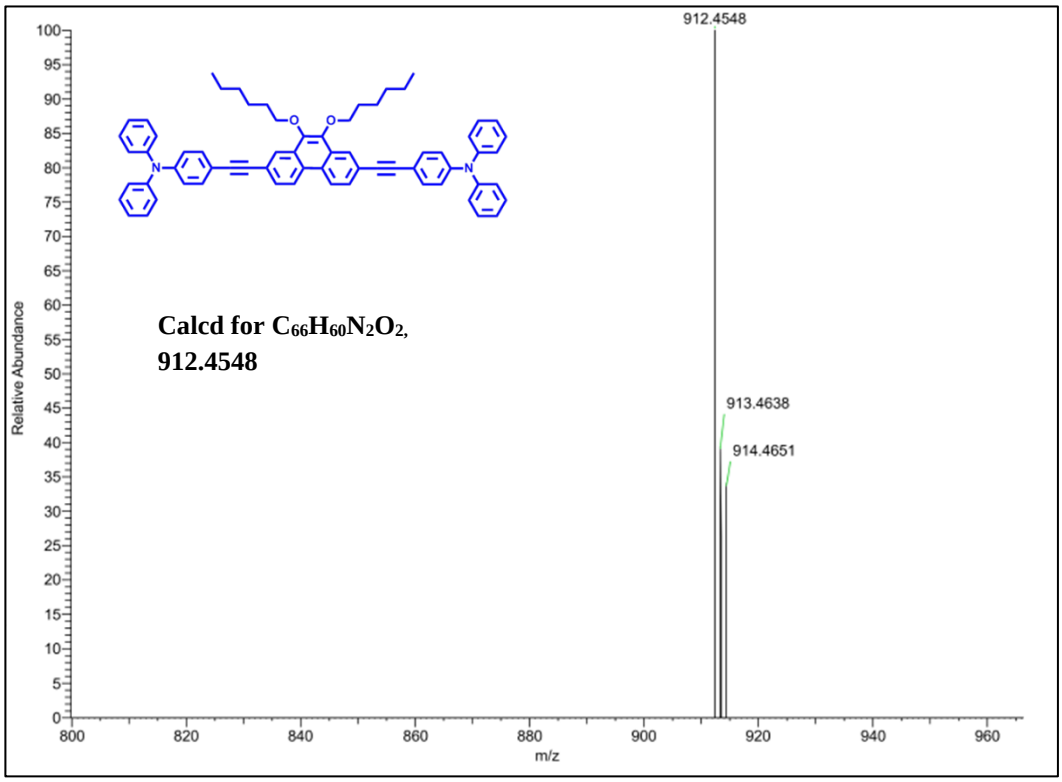

Figure S18: HRMS spectrum of compound 12b

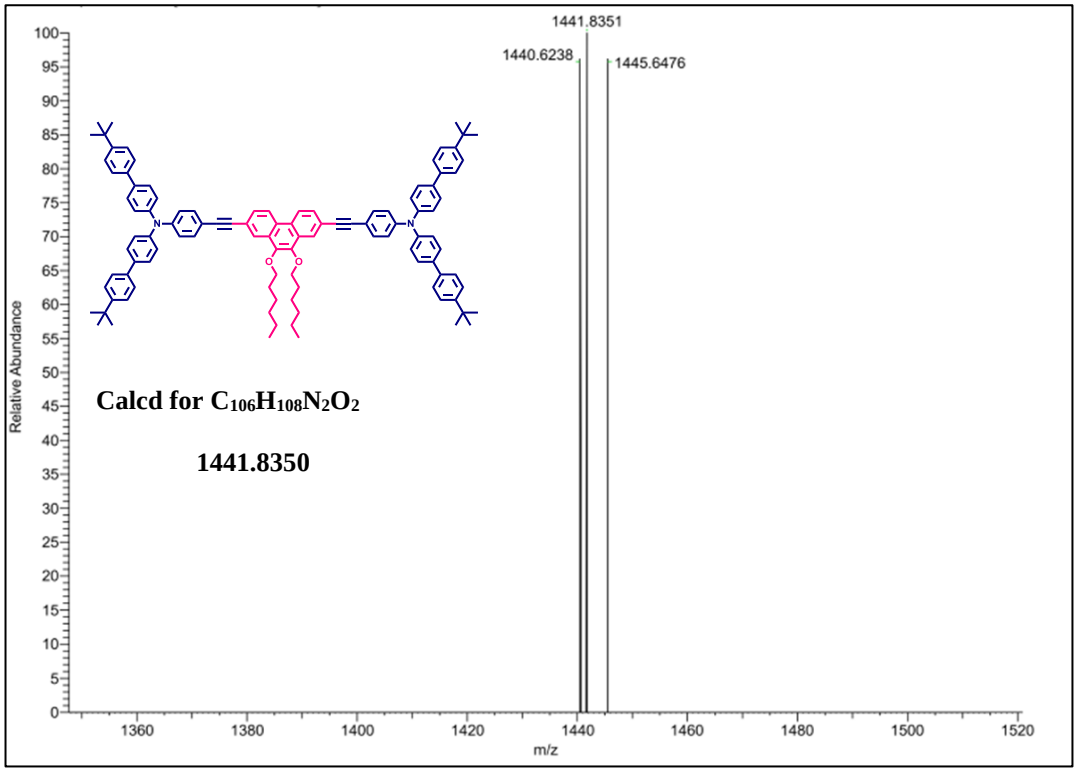

Figure S19: HRMS spectrum of compound 12c

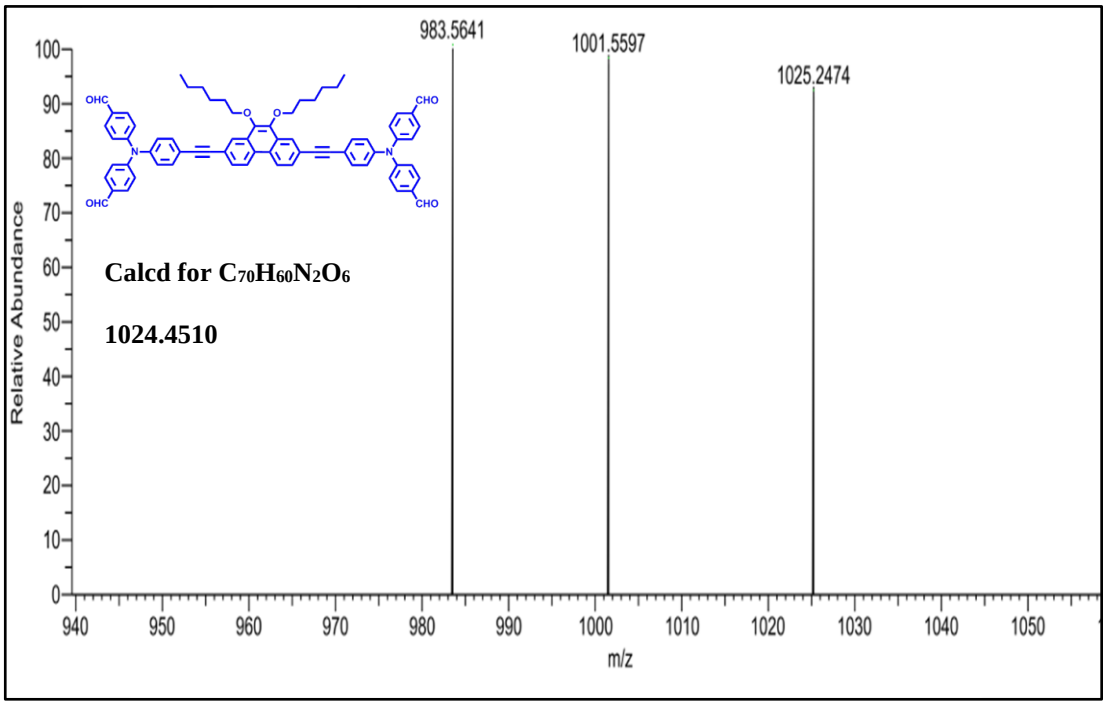

Figure S20: HRMS spectrum of compound 12d

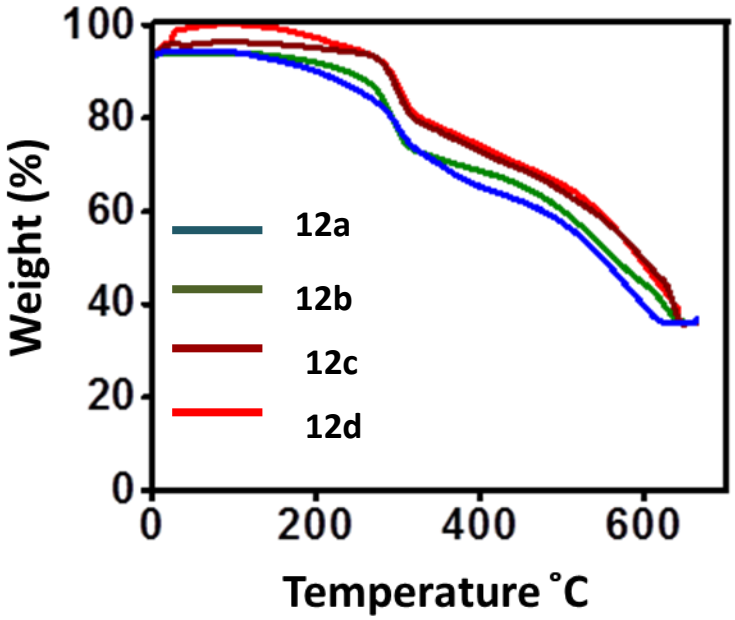

Figure S21: TGA curves of compounds 12a-d

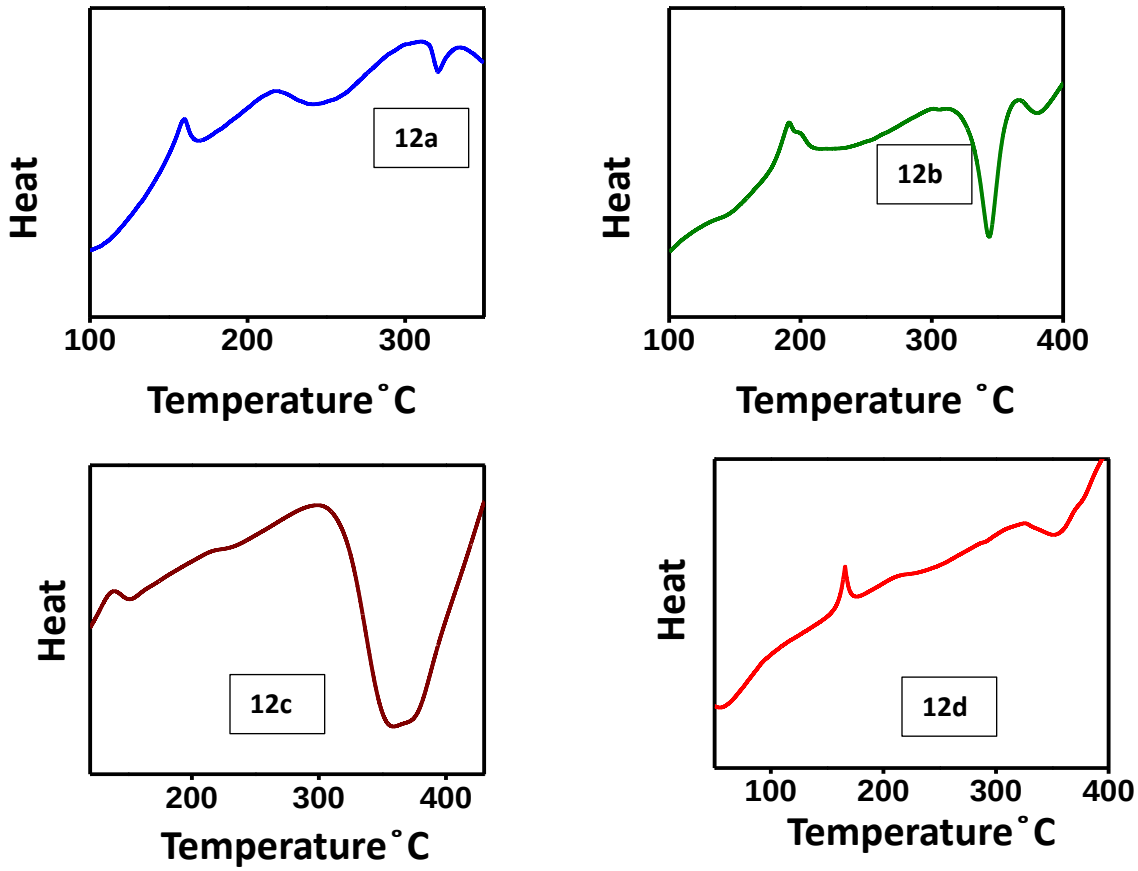

Figure S22: DSC thermograms of compounds 12a-d

Table S1: Thermal properties of compound 12a-d

12	T_g (°C)	T_m (°C)	T_d (°C)
a	160	320	333,502
b	191	344	345, 525
c	137	355	367,560
d	165	352	360, 545

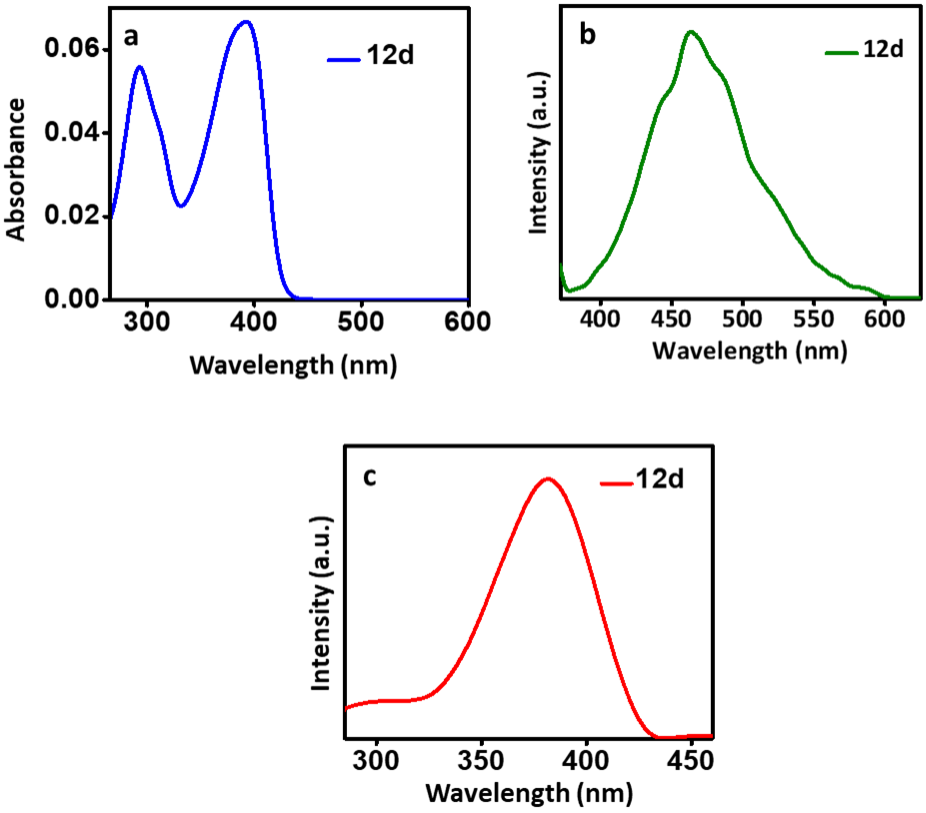

Figure S23: a) Absorption, b) emission and c) excitation spectra of compound 12d

Calculation of Marcus-Hush parameters for the rate of charge hopping: The rate constant for charge transfer (k) and, hence, the mobility is modeled by classical Marcus theory, where t is the transfer integral, is the reorganization energy, k_B is the Boltzmann constant, and T is the temperature. The reorganization energy λ_h or λ_e for hole or electron transfer, respectively, is calculated as the sum of the energy required for reorganization of the vertically ionized neutral to the cation or anion geometry, plus the energy required to reorganize the cation or anion geometry back to the neutral equilibrium structure on the ground-state potential energy surface.[4] For high charge carrier mobility, the reorganization energy needs to be minimized. The transfer integral depends on the relative arrangement of the molecules in the solid state and describes the intermolecular electronic coupling, which needs to be maximized to achieve high charge carrier mobility. λ_h = (E_{cation}(neutral geometry) - E(neutral)) + ($E_{neutral}$(cation geometry) - E(cation)) To calculate reorganization energy, four geometry optimization calculations were performed on a molecule to find the neutral ground state of the molecule ($E_{neutral}$), excited-state (anion) energy of the molecule on its ground state geometry (E_{anion}(neutral geometry)), excited-state geometry (E_{anion}) and neutral state energy of the molecule on its excited state geometry ($E_{neutral}$(anion geometry)). From these values, the Marcus rate for charge hopping is calculated by using the equation k = A2 /ħ * sqrt(π/(λ_hkBT)) * exp(-λ_h/(4kBT)). Here, k is the rate of hole transfer, and A is the charge transfer integral. kB is the Boltzmann constant. Due to the Arrhenius nature of dependence on reorganization energy, a lower value of λ_h would mean a marked increase in the charge hopping rate of the material. Table S2 shows the reorganization energy, transfer integral, and charge hopping rate of the compounds **12a-d**.

Table S2: DFT (631d) calculated parameters and hopping rates using Marcus-Hush theorem

Compounds	Reorganization value (DFT) λ_h [meV]	Effective charge transfer integral A [meV]	Charge hopping rate [S^{-1}] × 10^{13}
12a	119.73	6.49	2.257
12b	114.97	11.82	3.949
12c	100.68	17.29	5.510
12d	108.84	13.24	4.317

Computational Insights:

A series of computational simulations, such as molecular mechanics and semi-empirical methods, were used to study molecular packing and predict the electronic properties of the system. The geometrical parameters were used to compute the optimized structure at the DFT's B3LYP level of theory and TD-SCF for spectral estimation. The DFT calculations were performed with the Gaussian at the 6-31D level of theory. All the molecules were optimized by considering symmetry in effect. MedeA was used to calculate the bandgap, and the FMOs were visualized using Gaussview software. The optimized geometry was used as input for Density of States (DOS) calculations using VASP (MedeA, Materials Design, http://www.materialsdesign.com) software. The structures were evaluated involving solvent correction parameter GGA-PBE basis set.[5,6]

Fermi levels describe the probability of electrons occupying a certain energy state (**Table S2**). And also represents the availability of space for the movement of electrons, while the DOS presents the number of states which offer high space for particle movements (**Table S3**, **Figure S24**). The hopping values were then found to account for non-covalent interactions that should stabilize the packing pattern. This packing allows observing the stacking factor as well. The space groups were chosen to represent the plausible crystalline structure. While some inter-atomic distances were monitored and measured below 10 Å, which

are the significant ones. Optimized geometry with the dihedral angles represented in **Figure S25.** It visualizes relatively planar structures for all compounds. Furthermore, the data indicates that backbone distortions from planarity in these compounds occur only between the central phenanthrene core and end-capping units, with minimum torsional angles varying from 7 to 44°. This ensures the compounds do not change their planarity due to the various electronic substitutions. Instead, they have induced non-covalent interactions, which assisted the OFET performance.

It has been found that the hopping distances are favorable enough for non-bonding interactions between "heteroatoms" and π-π type transitions. However, compounds **12b** and **12c** are connected with triphenylamine and tert-butylphenyl triphenylamines respectively, which could substantiate the suitable charge transport properties. Various symmetry structures were tried to get packing patterns, in which closer interaction and stabilization were found with the respective symmetry mentioned in **Table S3** and **Figure S26**. For instance, molecules **12b** and **12c** have shown P21 and P212121 symmetry with which the structure appears to present a solid packing with more stabilization due to inter-atomic interaction with corresponding hetero atoms. The higher molecular symmetries allowed molecular packing in a favorable pattern for inter-molecular interaction and supported the polymorphic structure. Such a packing with minimum repulsion and maximum interaction with plenty of orbitals makes this molecule suitable for molecular semiconducting devices, comparatively.

Table S3: Crystalline parameters of compounds 12a-d

12	**Cell Parameters** a / b / c α / β / γ	**Type of Cell**	**Preferences**	**Symmetry**	**Hopping Distances** Å
a	24.5/15.6/25.7 90/90/90	simple orthorhombic	2 1 2	P212121	2.782 6.767 8.887
b	18.9/8.79/34.6 90/90/90	simple orthorhombic	2 2 2	P21	2.717 5.406 6.199
c	42.1/25.8/17.3 90/90/90	simple orthorhombic	1 2 1	P212121	2.610 4.316 9.704
d	18.3/35.4/16.4 90/90/90	simple orthorhombic	2 3 1	P-1	8.459 8.666 8.742

Table S4: Fermi energies and DOS gaps of compounds 12a-d

12	Molecular Formula	Free Energy (eV)	Density (Mg/m^3)	DOS Gap (eV)	E Fermi (eV)	Dipole D	Symmetry
a	$C_{82}H_{96}O_6$	-589.66	0.250	-2.2436	-4.245	1.556	Cs
b	$C_{66}H_{60}N_2O_2$	-543.48	0.736	-1.7374	-2.784	2.288	C_2V
c	$C_{106}H_{108}O_2N_2$	-500.47	0.288	-2.3034	-4.437	0.469	C_2
d	$C_{70}H_{60}O_6N_2$	-676.27	0.564	-2.3551	-3.733	2.335	Cs

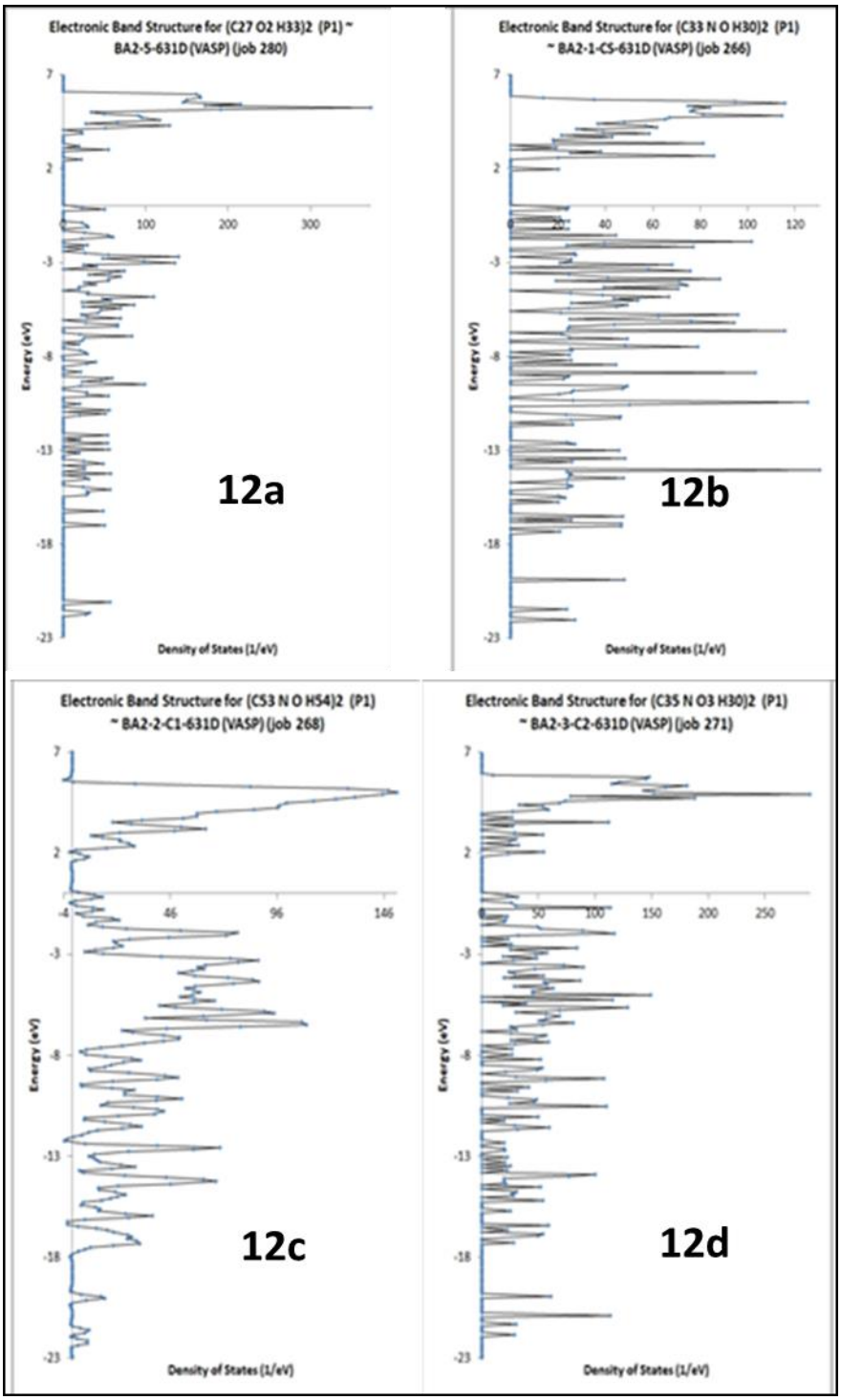

Figure S24: DOS graphs of compounds 12a-d

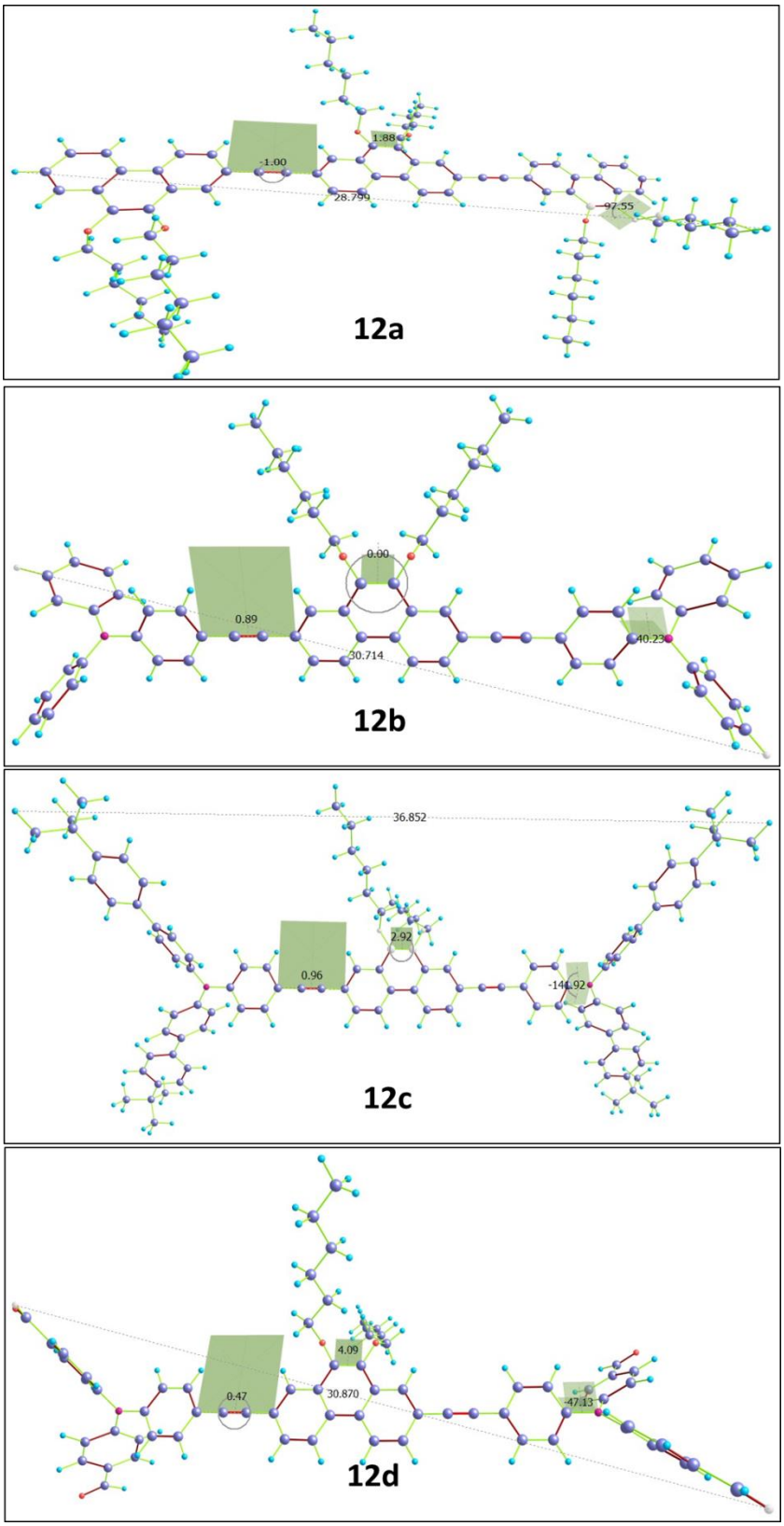

Figure S25: Optimized geometry and dihedral angles of compounds 12a-d

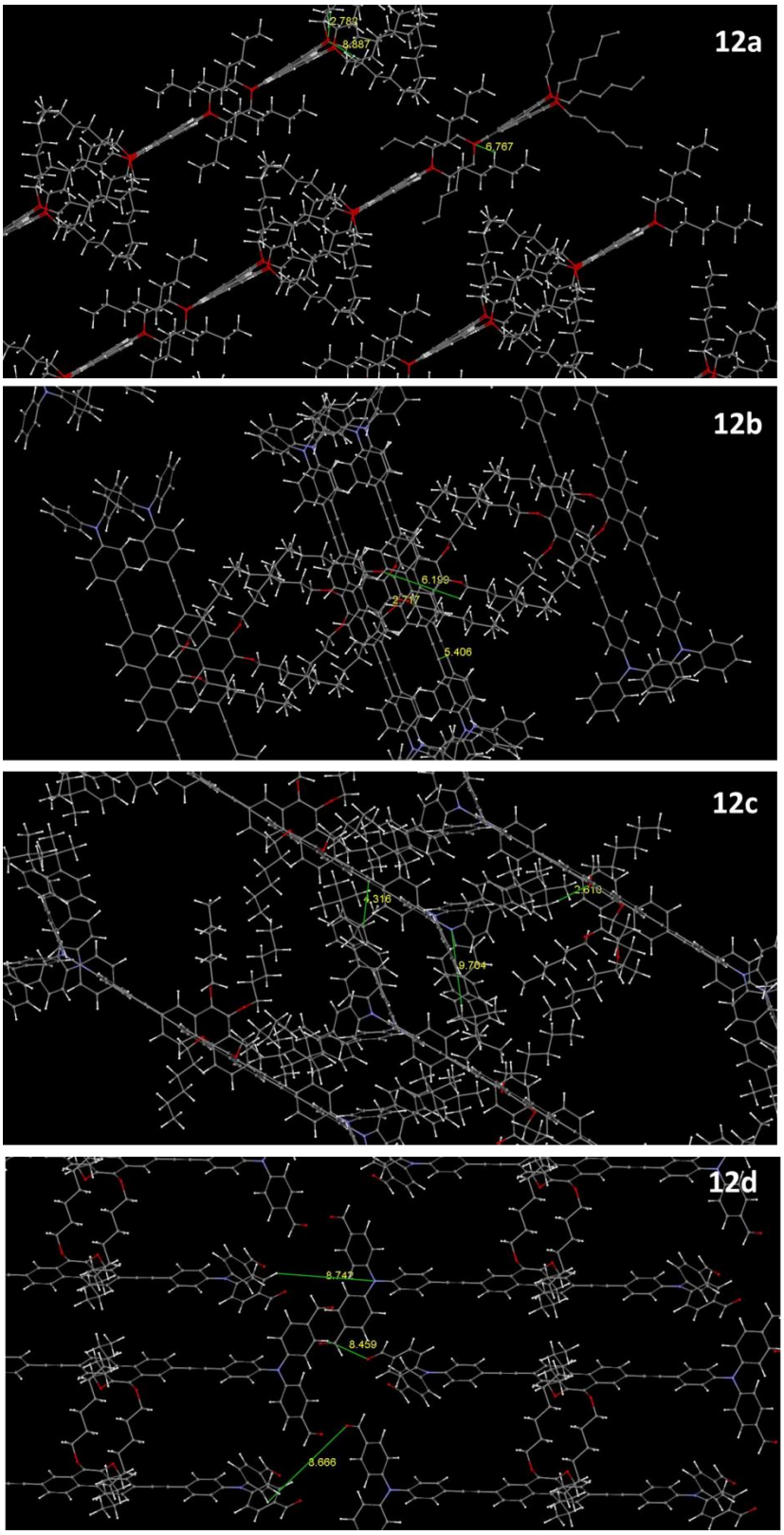

Figure S26: Packing pattern of compounds 12a-d

TDDFT studies:

Time-dependent Excited states of this series of molecules are calculated by the computational method and are compared favorably with experimentally obtained values.[7] The theoretical calculations using the TD-SCF (Time-Dependent SCF) suggest significant spectral insights. The bands found in the experimental methods are quite in agreement with the theoretical calculations. Also, the emission spectral values are quite predictable. Theoretical understanding of electronic absorption and emission energies of a series of phenanthrene based compounds through an assessment of several TDDFT functionals and a detailed study of solvent effects on their ground and excited state structures and properties are calculated and shown in **Table S5** shows the comparison of the several values predicted by the theoretical methods only four values have been chosen that are closer to the experimental ones and that have a good frequency factor.

Table S5: Electronic absorption behavior of compounds 12a-d by TDDFT

12	Wavelength (nm)	Electronic transition
	458.75	S_2-T_4
a	390.68	S_0-S_1
	361.09	S_3-S_1
	360.11	S_2-S_1
	446.23	S_2-T_2
b	439.89	S_0-S_1
	416.57	S_1-S_1
	401.46	S_2-S_1
	585.38	S_0-S_1
c	519.14	S_1-T_1
	455.95	S_0-S_1
	419.50	S_1-S_1
	495.93	S_1-T_2
d	447.13	S_0-S_1
	440.73	S_0-S_3
	432.01	S_0-S_2

The time dependent extension TDDFT, has also received wider acclaim for the excitation energy calculations of electronically excited states. Although TDDFT enjoys huge success, it carries its drawbacks as it underestimates long-range charge transfer excitation energies. The inter-system crossing has been predicted in almost all the systems and some of the values of emission Spectra agree with these values. These are the states where excited electrons may be promoted to account for the spectral and conducting properties of the molecule. The TDDFT calculations also show various such states within the experimentally measured values. Among the transitions predicted, S_0-S_1 transitions calculated which much similar to the experimental absorption values. This way. The molecules 12a-d show numerous levels, especially molecule **12a** and **12c** showing many numbers of triplet states. The high fluorescence nature of the compound also supports these results.[8,9]

OFET device fabrication and characterization

OFETs based on four new phenanthrenes (**12a-d**) were fabricated using heavily n^{++} doped silicon wafer in bottom-gate top contact (BGTC) architecture. Initially, silicon wafers were ultrasonically cleaned in acetone, methanol, and finally over a mild piranha solution. Subsequently, the silicon wafer was heated up to 1200 °C for 80 min to grow SiO_2 dielectric layer. The thickness of the thermally grown dielectric layer was ~ 300 nm and the silicon wafer functioned as a gate. The compounds (**12a-d**) were well-dissolved in chloroform (5 mg/ml) and sonicated for 20 minutes. This solution was layered over the SiO_2 dielectric layer by spin coating at 3000 rpm speed for one minute. Then the device was heated over a hot plate at 80 °C for 45 minutes to remove residual solvent. In addition, the wafer is thermally annealed at 90 °C for 30 min as a post-deposition treatment to attain better self-assembly. Then silver contacts were made as to the source and drain to complete the fabrication. The width and length of the channels were 5 mm and 150 µm, respectively.

Keithley 4200A SCS analyzer was used to investigate transistor characteristics. A probe station was utilized to source a voltage and to read back the associated current simultaneously. The SMUs were in turn connected to a probe station (Everbeing), which consist of three test probes, three triaxial wires, and micropositioners (made up of tungsten). A test probe is used in each one of the terminals (source, drain, and gate) of the transistor. Test probes could be adjusted in various directions with the micropositioners and allowed the measurements to characterize the OFETs.

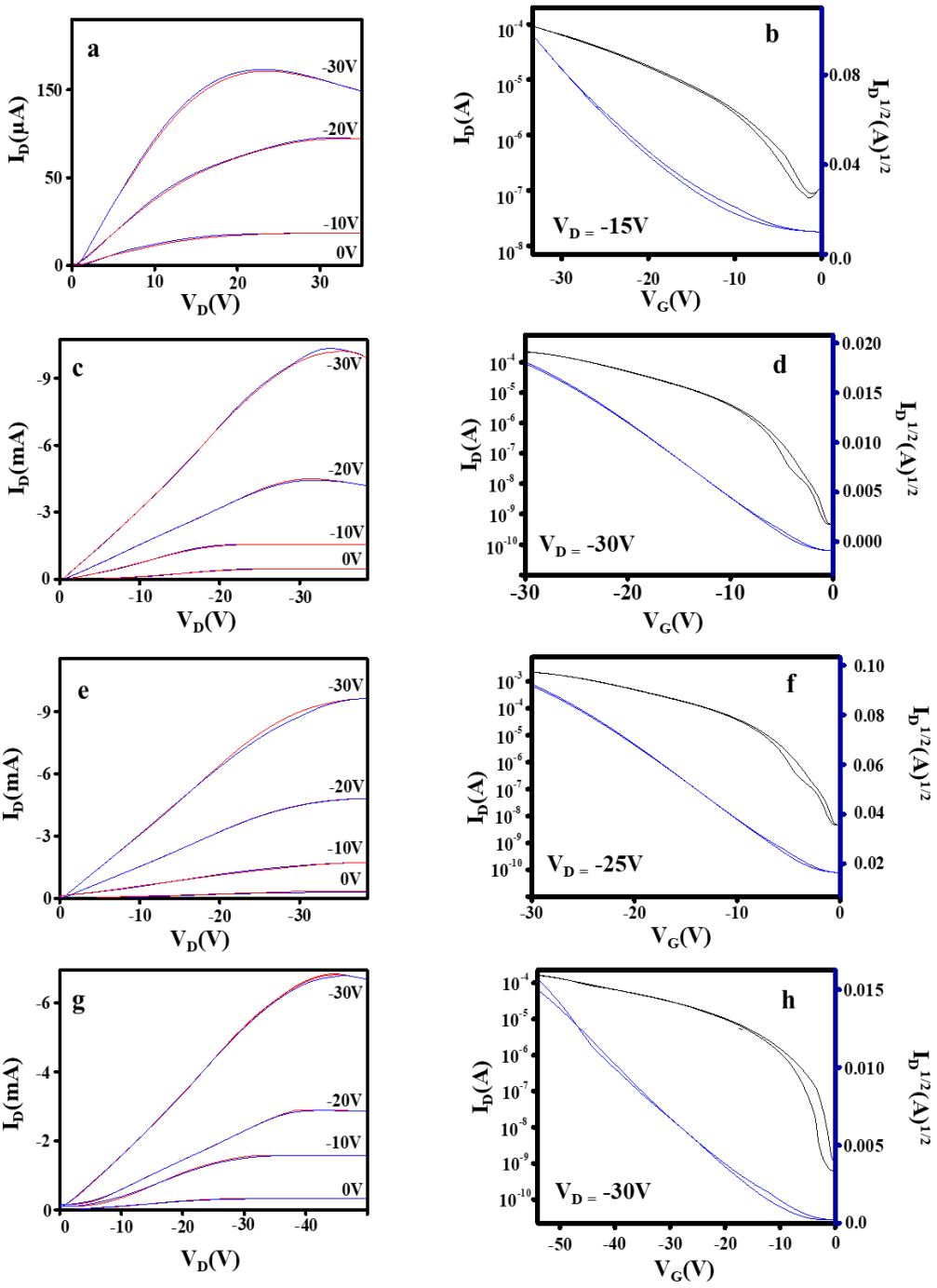

Figure S27: Hysteresis analysis of compounds 12a (a, b), 12b (c, d), 12c (e, f), 12d (g, h) by forward and backward scans

Table S6: PVA dielectric based OFET characteristics of compounds 12a-d

12	Mobility μ_h (cm^2/Vs)[a]	$I_{on/off}$	Threshold voltage (V)
a	1.8±0.02	10^4	-5
b	2.9±0.05	10^6	-6
c	3.4±0.04	10^8	-4
d	3.1±0.03	10^7	-4

a. The error bar calculated from five devices

Table S7: PMMA dielectric based OFET characteristics of compounds 12a-d

12	Mobility μ_h (cm^2/Vs)[a]	$I_{on/off}$	Threshold voltage (V)
a	1.5±0.02	10^4	-5
b	2.6±0.05	10^6	-5
c	3.5±0.04	10^7	-4
d	3.2±0.03	10^7	-4

b. The error bar calculated from five devices

Simulated XRD analysis

Crystal Sleuth software and material studio software[10] to estimate that diffraction line shows that the values at the peaks are consistent with the described values, the XRD configuration acquired from the fabricated **12d** thin film had matching corresponding to observe, calculate and difference of the crystal system, 2 theta values are presented in **Table S8.**

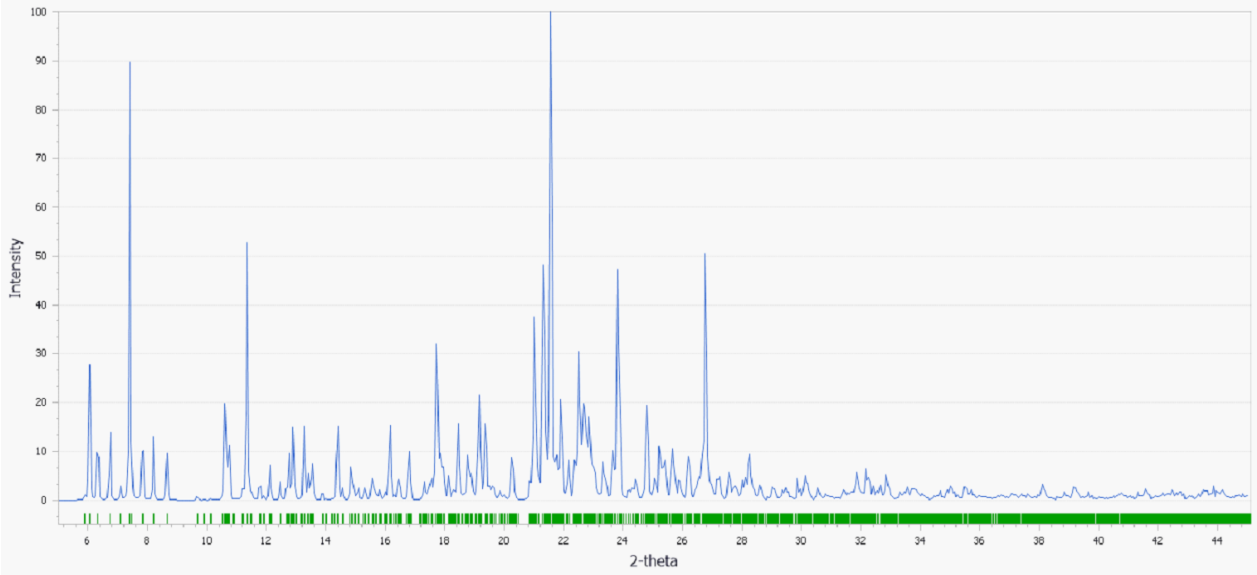

Figure S28: Simulated XRD pattern of compound 12d

Table S8: Comparison of experimental and simulated XRD data of compounds 12a-d

Compound	2Θ Experimental	2Θ DFT
12a	7.01 10.67 14.26 20.18 23.59	6.09 10.35 14.98 21.3 24.12
12b	7.03 8.29 9.93 14.08 21.70 22.44 23.41 26.52 30.85 32.44	7.59 8.56 10.52 13.95 21.80 23.54 24.41 26.52 30.85 33.45
12c	6.64 12.50 13.72 14.57 15.79 22.13 24.57 30.18 34.32 35.67	6.90 13.50 13.95 14.54 15.32 22.17 25.40 30.57 35.40 36.51
12d	6.28 7.74 11.03 13.78 16.15 19.08 20.18 23.90	6.90 7.89 11.20 13.32 16.35 19.23 21.0 22.90

References:

[1] C. Monterde, R. Navarro, M. Iglesias, F. Sánchez, **n.d.**, 1–43.

[2] A. Anjali, P. M. Imran, N. S. P. Bhuvanesh, S. Nagarajan, *Macromol. Rapid Commun.* **2022**, *43*, 2100472.

[3] A. Broggi, I. Tomasi, L. Bianchi, A. Marrocchi, L. Vaccaro, *Chempluschem* **2014**, *79*, 486–507.

[4] K. Patrikar, N. Jain, D. Chakraborty, P. Johari, V. R. Rao, D. Kabra, *Adv. Funct. Mater.* **2019**, *29*, 1805878.

[5] J.-L. Brédas, J. P. Calbert, D. A. da Silva Filho, J. Cornil, *Proc. Natl. Acad. Sci.* **2002**, *99*, 5804–5809.

[6] M. Fahlman, S. Fabiano, V. Gueskine, D. Simon, M. Berggren, X. Crispin, *Nat. Rev. Mater.* **2019**, *4*, 627–650.

[7] M. Oltean, A. Calborean, G. Mile, M. Vidrighin, M. Iosin, L. Leopold, D. Maniu, N. Leopold, V. Chiş, *Spectrochim. Acta Part A Mol. Biomol. Spectrosc.* **2012**, *97*, 703–710.

[8] P. Devibala, B. Balambiga, P. Mohamed Imran, N. S. P. Bhuvanesh, S. Nagarajan, *Chem. Eur. J.* **2021**, *27*, 15375–15381.

[9] R. Dheepika, A. Shaji, P. M. Imran, S. Nagarajan, *Org. Electron.* **2020**, *81*, 105568.

[10] A. A. I. Abd-Elmageed, A. F. Al-Hossainy, E. M. Fawzy, N. Almutlaq, M. R. Eid, A. Bourezgui, S. M. S. Abdel-Hamid, N. B. Elsharkawy, M. Zwawi, M. H. Abdel-Aziz, *Opt. Mater. (Amst).* **2020**, *99*, 109593.